*J Neurophysiol* 95: 1588–1607, 2006.
First published December 7, 2005; doi:10.1152/jn.00318.2005.

# Eye Movements of the Murine P/Q Calcium Channel Mutant *Tottering*, and the Impact of Aging

**John S. Stahl,[1,2] Robert A. James,[1] Brian S. Oommen,[2] Freek E. Hoebeek,[3] and Chris I. De Zeeuw[3]**
[1]*Department of Neurology, Case Western Reserve University, Cleveland;* [2]*Department of Neurology, Louis Stokes Cleveland Department of Veterans Affairs Medical Center, Cleveland, Ohio; and* [3]*Department of Neuroscience, Erasmus Medical Center, Rotterdam, The Netherlands*

Submitted 28 March 2005; accepted in final form 2 December 2005

**Stahl, John S., Robert A. James, Brian S. Oommen, Freek E. Hoebeek, and Chris I. De Zeeuw.** Eye movements of the murine P/Q calcium channel mutant *tottering*, and the impact of aging. *J Neurophysiol* 95: 1588–1607, 2006. First published December 7, 2005; doi:10.1152/jn.00318.2005. Mice carrying mutations of the gene encoding the ion pore of the P/Q calcium channel (Cacna1a) are an instance in which cerebellar dysfunction may be attributable to altered electrophysiology and thus provide an opportunity to study how neuronal intrinsic properties dictate signal processing in the ocular motor system. P/Q channel mutations can engender multiple effects at the single neuron, circuit, and behavioral levels; correlating physiological and behavioral abnormalities in multiple allelic strains will ultimately facilitate determining which alterations of physiology are responsible for specific behavioral aberrations. We used videooculography to quantify ocular motor behavior in *tottering* mutants aged 3 mo to 2 yr and compared their performance to data previously obtained in the allelic mutant *rocker* and C57BL/6 controls. *Tottering* mutants shared numerous abnormalities with *rocker*, including upward deviation of the eyes at rest, increased vestibuloocular reflex (VOR) phase lead at low stimulus frequencies, reduced VOR gain at high stimulus frequencies, reduced gain of the horizontal and vertical optokinetic reflex, reduced time constants of the neural integrator, and reduced plasticity of the VOR as assessed in a cross-axis training paradigm. Unlike *rocker*, young *tottering* mutants exhibited normal peak velocities of nystagmus fast phases, arguing against a role for neuromuscular transmission defects in the attenuation of compensatory eye movements. *Tottering* also differed by exhibiting directional asymmetries of the gains of optokinetic reflexes. The data suggest at least four pathophysiological mechanisms (two congenital and two acquired) are required to explain the ocular motor deficits in the two Cacna1a mutant strains.

## INTRODUCTION

The exact role the vestibulocerebellum plays in eye movement control remains unresolved. Many investigators have commented on the unusual anatomical, cytoarchitectural, and electrophysiological features of the cerebellum and reflected that the degree to which these features have been conserved through evolution indicates they are vital to the structure's overall computational role. One of these striking features is the Purkinje cell's interdependent calcium and potassium conductances, which enable even the most distal inputs to the enormous dendritic arbor to influence the axonal firing rate (De Schutter and Bower 1994; Jaeger et al. 1997; Llinas and Sugimori 1980), while at the same time providing a mechanism whereby the spread of synaptic potentials can be tightly restricted (Llinas and Moreno 1998). There is a consensus that these currents are critical to the Purkinje cell's function. Nevertheless, the currents' contribution, in computational terms, remains elusive (Yuste and Tank 1996). We have previously observed that a potential approach to the problem is to study mice carrying mutations predicted to alter Purkinje cell electrophysiology, and we chose to study strains bearing mutations of Cacna1a, the gene encoding the ionophore subunit of the P/Q-type calcium channel (Stahl 2002, 2004a). This channel is the primary determinant of calcium currents in the Purkinje cell dendrite (Llinas et al. 1989), participates in synaptic transmission at several points in the vestibulocerebellar circuitry, and mouse strains bearing Cacna1a mutations all suffer varying degrees of motor impairment customarily interpreted as cerebellar in origin (Ashcroft 2000; Zwingman et al. 2001).

The inherent problem in studying such mutants, however, is that the P/Q calcium channel is expressed at several points within regions of the brain participating in control of eye movement. As such, one cannot attribute any specific behavioral finding a priori to deranged Purkinje cell dendritic integration. Even if one assumes the dysfunction is localized to the cerebellar cortex (and there are reasons to accept this assumption as a working hypothesis; see DISCUSSION), it would remain unknown whether the dysfunction stems directly from altered P/Q calcium currents or from secondary changes induced by the abnormal currents. For instance, the Cacna1a mutation in the *tottering* strain results in an increased dependency on N-type, rather than P/Q-type, calcium channels at the synapses of parallel fibers on Purkinje cells (Zhou et al. 2003), and the shift was predicted to render these synapses more susceptible to the inhibitory effects of cortical interneurons. A relative sparing of inhibitory compared with excitatory neurotransmission (Caddick et al. 1999) and climbing fiber as opposed to parallel fiber synaptic efficacy (Matsushita et al. 2002) have also been reported in this strain. Such secondary effects would ultimately disrupt the normal balance of inputs to the Purkinje cell. Reduced P/Q channel conductivity may also trigger alterations in mechanisms of intracellular calcium homeostasis and thereby alter processes in which calcium acts as a second messenger, such as long-term depression or nitric oxide generation (Cicale et al. 2002; Dove et al. 2000; Murchison et al. 2002; Rhyu et al. 2003).

Address for reprint requests and other correspondence: J. Stahl, Dept. of Neurology, University Hospitals of Cleveland, 11100 Euclid Avenue, Cleveland, OH 44106-5040 (E-mail: jss6@po.cwru.edu).

The costs of publication of this article were defrayed in part by the payment of page charges. The article must therefore be hereby marked "*advertisement*" in accordance with 18 U.S.C. Section 1734 solely to indicate this fact.

Because the Cacna1a mutation is expressed throughout the life of the animal, it could also potentially alter the development and maintenance of the ocular motor circuits. Detailed anatomical studies of the ocular motor circuitry in Cacna1a mutants have not been undertaken, although even if such studies were to confirm the gross integrity of these pathways, they still could not exclude the possibility that there are quantitative changes at the ultrastructural level (e.g., shape of dendritic arbors or density and distribution of synaptic contacts) that influence signal processing. An instance of such ultrastructural changes has, in fact, been described (Rhyu et al. 1999). Finally, it should be recognized that Cacna1a mutations can have diverse effects even at the level of the P/Q calcium channel itself. This point is demonstrated by studies of CACNA1A mutations associated with a human channelopathy disorder, familial hemiplegic migraine (FHM). When expressed in cultured granule cells, P/Q calcium channels incorporating FHM mutations exhibit decreased unitary calcium currents, but more hyperpolarized activation voltages, resulting in increased open-channel probability and thus *increased* single-channel calcium influx over a large voltage range (Tottene et al. 2002). At the same time, the mutation results in lower channel density, which reduces the total maximal P/Q calcium current. The multiplicity of effects on the P/Q calcium channel renders it more difficult to prove causal relationships between a specific biophysical aberration, alterations of neuronal signal processing, and a given behavioral abnormality.

One approach to unraveling these uncertainties involves studying each Cacna1a mutant strain over a broad range of ages. Abnormalities that appear and progress through life should originate in structural or electrophysiological properties that are similarly progressive. Conversely, progressive behavioral abnormalities are unlikely to stem *directly and/or exclusively* from a stationary change in channel biophysics. A related strategy involves studying several different Cacna1a mutants, with special attention to identifying behavioral abnormalities whose severity varies across strains. Provided that qualitatively similar behavioral abnormalities stem from the same pathophysiological mechanism, the severity of the behavioral abnormalities should covary with the severity of that causal biophysical, structural, or electrophysiological derangement. Conversely, biophysical, structural, or electrophysiological aberrations that do not covary with the severity of the behavioral abnormality are less likely to be *directly* responsible for that behavioral abnormality. Thus comparisons across allelic strains can be used to generate hypotheses regarding the causes of ocular motor abnormalities in Cacna1a mutants, and in turn, lead to insight into the connection between a particular biophysical, structural, or systems property and the normal function of the vestibulocerebellum.

To date, geneticists have identified seven murine Cacna1a mutants. Listed in rough ascending order of ataxia severity, the strains are: *rocker*, *tottering*, *tottering-4J*, *tottering-5J*, *rolling-Nagoya*, *tottering-3J*, and *leaner* (Zwingman et al. 2000, 2001). Although some of these strains exhibit prominent age-related cerebellar degeneration, histology in others (i.e., *rocker*, *tottering*, *tottering-4J*, and *tottering-5J*) is relatively normal (Zwingman et al. 2000, 2001), and thus behavioral abnormalities may stem from congenitally altered channel biophysics rather than from loss of neuronal elements. *Rocker* (*rkr*) and *tottering* (*tg*) are particularly convenient for these studies because of the topographical similarity of their mutations (single amino acid substitutions in homologous extracellular loops adjacent to the mouth of the ionophore) and the fact that the animals are robust, with normal life span and fecundity. Our previous study of *rocker* revealed ocular motor abnormalities that are consistent with interference with functions that have been attributed to the cerebellar flocculus of afoveate mammals (Stahl 2004a). Some of these abnormalities appeared to be congenital, such as subnormal gains of the vestibuloocular reflex (VOR) and visually augmented vestibuloocular reflex (VVOR), abnormally large VOR phase leads at low stimulus frequencies, deficient plasticity of VOR geometry, and slowing of fast phases of vestibular nystagmus. Other abnormalities appeared or clearly progressed with age, including subnormal gain of the optokinetic response (OKR) and static hyperdeviation of the eyes. In the current study we assessed the integrity of the same ocular motor functions in *tottering*, comparing this strain to both *rocker* and control animals of the reference inbred strain C57BL/6, on which background the *rocker* and *tottering* mutations have been maintained. In addition, we conducted analyses in all three strains of additional functions not assessed in the previous report, including the time constant of the brain stem neural integrator, axis of the ocular response to rapid pulses of head velocity ("thrusts"), and speed tuning of the vertical OKR. Preliminary reports have been published (Stahl 2004b; Stahl and James 2003, 2004, 2005).

## METHODS

### *Animals and animal preparation*

Experimental use of mice was approved by the Institutional Animal Care and Use Committee at Case Western Reserve University and conformed to the National Institutes of Health guidelines for the use and care of vertebrate animals. Homozygous *tottering* mutants were obtained by crossing animals doubly heterozygous for the closely linked *tottering* and oligosyndactylism mutations (i.e., +Tg/Os+ × +Tg/Os+), resulting in only new double heterozygotes and *tottering* homogyzotes (TgTg/++), the ++/OsOs genotype being lethal in utero (Isaacs and Abbott 1992). The *tottering* homozygote progeny are recognizable by their ataxic gaits and normal (nonfused) digits. Colony founders were originally generated by crossing *tottering* homozygotes maintained on a C57BL/6 background with leaner/Os double heterozygotes (B6.Cg-*Os* +/+ *Cacna1a*$^{tg\text{-}la}$/J) obtained from The Jackson Laboratory (Bar Harbor, ME). Comparative data for *rocker* and C57BL/6 control animals were drawn from our earlier study of *rocker* (Stahl 2004a), augmented by new data from C57BL/6J animals purchased from The Jackson Laboratory and studied concurrently with the *tottering* mutants. *Tottering* animals were aged 109–808 days at the time of eye movement recording. Overall, data described herein were collected from 28 *tottering*, 14 *rocker*, and 41 control animals. As in the previous study (Stahl 2004a), animals were divided into three age groups: 2–8 mo, 8–14 mo, and >14 mo. These groupings correspond roughly to breeding adult, late-breeding adult, and elderly periods for the laboratory mouse. *Tottering* recordings were planned so that the average ages of the animals within each age group were separated by about 6 mo. Some animals were recorded repeatedly and contributed to the database for more than one group (usually two). All animals did not undergo all types of testing. Numbers of animals tested in each condition and age group, as well as the average age of the animals tested in a particular condition, are summarized in Table 1.

Animals were housed in conventional (not microbially isolated) cages, segregated by sex, and exposed to a 12-h light/12-h dark

TABLE 1. *Numbers of animals and average ages for each tested ocular motor behavior*

| Condition | Age Group, months | Control N | Control Age, days | *Rocker* N | *Rocker* Age, days | *Tottering* N | *Tottering* Age, days |
|---|---|---|---|---|---|---|---|
| Static elevation | 2–8 | 10 | 103 | 7 | 125 | 13 | 131 |
| | 8–14 | 20 | 304 | 10 | 320 | 11 | 343 |
| | >14 | 13 | 466 | 9 | 520 | 10 | 622 |
| Fast phase dynamics | 2–8 | 29 | 91 | 7 | 125 | 12 | 137 |
| | 8–14 | 15 | 300 | 10 | 319 | 10 | 358 |
| | >14 | 13 | 463 | 9 | 537 | 10 | 623 |
| VOR/VVOR | 2–8 | 11 | 95 | 7 | 125 | 13 | 131 |
| | 8–14 | 13 | 303 | 10 | 321 | 11 | 343 |
| | >14 | 13 | 465 | 9 | 518 | 10 | 622 |
| Horizontal OKR | 2–8 | 20 | 76 | 5 | 130 | 13 | 131 |
| | 8–14 | 16 | 297 | 8 | 321 | 11 | 343 |
| | >14 | 13 | 468 | 7 | 485 | 10 | 622 |
| Vertical OKR | 2–8 | 12 | 105 | 4 | 180 | 12 | 158 |
| | 8–14 | — | — | 3 | 316 | 9 | 374 |
| | >14 | 11 | 475 | 5 | 514 | 10 | 632 |
| Thrusts | 2–8 | 14 | 100 | 8 | 136 | 14 | 116 |
| | 8–14 | 12 | 307 | 9 | 323 | 10 | 330 |
| | >14 | 13 | 463 | 9 | 526 | 11 | 614 |
| Cross-axis adaptation | 2–8 | 7 | 87 | 5 | 183 | 12 | 158 |
| | 8–14 | 12 | 356 | 8 | 366 | — | — |
| | >14 | 11 | 475 | 6 | 510 | — | — |
| Integrator time constant | 2–8 | 14 | 103 | 8 | 136 | 15 | 121 |
| | 8–14 | 12 | 306 | 10 | 320 | 11 | 331 |
| | >14 | 13 | 463 | 9 | 515 | 10 | 619 |

illumination cycle. Animals were prepared for eye movement recording by surgical implantation of an acrylic head-fixation pedestal as previously described (Stahl et al. 2000). To improve animal-to-animal consistency of pedestal placement, the surgery was performed with the animal in a stereotactic frame. Using a small probe held in a micromanipulator, we assessed the alignment of the stereotactic rostrocaudal axis with the animal's sagittal suture and adjusted the animal's yaw as necessary. We also determined the pitch angle of the lambda–bregma axis, and constructed the pedestal so that its top surface paralleled this axis. The holder used during recordings would place the pedestal surface (and thus the lambda–bregma axis) at a pitch-down angle of 18°. Before each recording session, the eye to be recorded was treated with an ophthalmic solution of 0.5% physostigmine salicylate to limit pupil dilation in darkness (Stahl 2002).

### *Eye movement recording and calibration*

Eye movement recordings were obtained from restrained, head-fixed animals using video-tracking methods as previously introduced (Stahl et al. 2000) and subsequently refined (Stahl 2002, 2004a). We regularly ensured that the videooculography vertical corresponded to Earth vertical by imaging a machinist's square or a miniature plumb bob arrangement mounted on the turntable, and adjusted the camera roll until the image of the reference fixture aligned perfectly with a vertical reference generated by the oculography system. This adjustment was particularly important for measuring the angle of the response to the thrust stimulus described below. Video images of either the left or right eye were processed by a commercial pupil tracker (ETL-200, ISCAN, Burlington MA), which extracted signals proportional to the horizontal and vertical (linear) positions of the pupil and reference corneal reflection (CR), as well as horizontal pupil diameter. Sampling rates were 240 Hz during measurements of nystagmus fast phases and 120 Hz for all other purposes. Note that the corresponding sampling rates for the control and *rocker* data derived from the previous study were 120 and 60 Hz, respectively. Analog outputs of the eye tracker were passed through four-pole Bessel low-pass filters (corner frequency 100 Hz), resampled at 200 Hz, and recorded on a PC-type computer. Other analog signals, including turntable position, optokinetic drum velocity, and planetarium velocity were similarly filtered, sampled, and stored.

The positions of pupil and CR were converted off-line to angular position as previously described (Stahl 2002, 2004a; Stahl et al. 2000). Briefly, we recorded the pupil and CR positions as the video camera was rotated over a 20° arc about an Earth-vertical axis passing approximately through the recorded eye. The positions obtained at the extremes of the camera rotation were used to calculate $R_P$, the linear distance between the center of the pupil and the center of corneal curvature in the Earth-horizontal plane passing through the pupil. Note that this distance decreases as the pupil assumes greater vertical elevations. We also determined the elevation-independent great circle radius $R_{P0}$, the distance between the center of the pupil and the centers of both vertical and horizontal corneal curvatures. Both $R_P$ and $R_{P0}$ were determined at various pupil diameters and linear regression performed to generate formulae relating these radii to pupil size. Horizontal or vertical eye-in-head angles ($E_H$, $E_V$) could then be determined in subsequent records by trigonometric formulae taking into account the linear pupil and CR positions and either $R_P$ or $R_{P0}$, adjusted for pupil size. The equation with $R_{P0}$ requires both the horizontal and vertical pupil and CR positions, and thus generates eye angles that are noisier than those generated by the $R_P$ equation, which is based on the horizontal channels alone. Thus the $R_{P0}$ equation was reserved for stimuli that generated appreciable vertical movements of the eye (i.e., the responses to the cross-axis and vertical OKR stimuli), which take the pupil away from the horizontal plane it occupied during calibration. The simpler formula based on $R_P$ and the horizontal pupil and CR positions was used for all other data. During assessments of absolute eye elevation at rest, we could assume the pupil lay at the same position that it occupied during the measurement of $R_P$. Thus the elevation above the ocular equator could be calculated using $R_P$ and the vertical linear distance between the pupil and CR centers ($\Delta Y$) according to the equation $E_V = \arctan(\Delta Y/R_P)$. During this measurement the reference IR emitter was moved from its customary position directly above the camera lens to the side of the camera lens. In this position there was no need to correct for the vertical separation of the reference emitter and the camera optical axis, which requires assumptions about the radius of corneal curvature (Stahl 2004a).

### *Stimulus apparatus and conditions*

All stimulus instruments were identical to those previously detailed (Stahl 2004a). Briefly, vestibular and optokinetic stimuli about an Earth-vertical axis were generated by a servo-controlled turntable and optokinetic drum, respectively. The calibration procedure guarantees that the rotational axis of the turntable runs through the center of the recorded eye, and the rotational axis of the drum is approximately aligned with that of the table. During cross-axis adaptation and assessment of vertical OKR (see following text), optokinetic stimuli about a rostrocaudal (roll) axis were generated by a projection planetarium (Leonard et al. 1988) mounted over the animal's head and projecting onto a featureless gray fabric background.

The majority of stimulus conditions used in this study were detailed previously (Stahl 2004a). The determination of average absolute vertical position was based on approximately 60 s of recording with the animal held motionless in the light. Horizontal nystagmus fast phases for analysis of peak velocity–amplitude relationships were generated by slowly rotating the animal under manual control in the light. VOR and VVOR were tested by rotating the animal in darkness and light, respectively, at 0.1 Hz, ±10° amplitude; 0.2 Hz, 10°; 0.4 Hz, 10°; 0.8 Hz, approximately 4.6°; and 1.6 Hz, approximately 3.9°. Corresponding velocity amplitudes were ±6, 13, 25, 23, and 39°/s. Both horizontal and vertical (roll axis) OKR were assessed during

constant-velocity rotations at ±2.5, 5, 10, 20, and 40°/s. Constant-velocity periods alternated direction, lasted 4 s each, and were separated by 3.5-s periods of darkness during which the drum/planetarium reversed direction and reaccelerated to the next test speed. The ability of the animal to alter the direction of its compensatory eye movements (cross-axis adaptation) was tested by oscillating the animal in the light at 0.4 Hz, 10° amplitude while simultaneously rotating the planetarium about an Earth-fixed rostrocaudal (roll) axis at the same frequency and amplitude. The phase of the planetarium rotation was adjusted with respect to the turntable so as to promote downward eye movements in association with nasally directed horizontal compensatory eye movements. VOR direction was assessed (in darkness) before adaptation, and then for a brief period every 10 min during a 50-min adaptation period. Samples of the response in the presence of the adaptation stimulus were also obtained at 10-min intervals.

Two types of measurements were not included in the previous study and thus are described here in more detail. The alignment of VOR response and stimulation axes was assessed in the light using 15°, steplike rotations of the turntable with peak velocities of approximately 110°/s and accelerations of 2200°/s$^2$ (a so-called thrust stimulus; Walker and Zee 1999). The speed was sufficient to guarantee that the ocular response was largely attributed to the VOR while not being so fast as to agitate the animals. In some control animals it was necessary to reduce the stimulus amplitude by 25% because at the standard stimulus amplitude the response was consistently interrupted by a fast phase. This study also assessed the time constant of the neural integrator. Animals were rotated slowly in the light to generate eccentric eye positions. Once an eccentric eye position had been achieved, rotation was halted for ≥2 s to allow the semicircular canals to partially reequilibrate. The lights were then extinguished and the subsequent centripetal drift of eye position was recorded.

### *Data analysis*

Analysis procedures for fast phases of vestibular nystagmus, VOR, OKR, and cross-axis adaptation were identical to those previously detailed (Stahl 2004a). Briefly, fast phases of vestibular nystagmus (henceforth loosely termed "fast phases") were quantified by linear regression of peak eye velocity versus fast phase amplitude, with the regression forced to pass through the origin. Horizontal eye velocities used in this analysis were calculated off-line by numerically differentiating the eye position signal after smoothing it by convolution with a Blackman window whose cutoff frequency was either 40 or 80 Hz. The lower value was used whenever data were to be compared with data collected in the previous study (Stahl 2004a), in which the lower video sampling rate also mandated a lower smoothing cutoff frequency. VOR and VVOR data were processed by Fourier analysis to extract gain and phase values with respect to head velocity. Gain versus frequency and phase versus frequency (Bode) plots were compiled for each recording session, curves from two or more sessions were averaged to generate a single Bode plot for each animal, and these single-animal curves were in turn averaged to generate curves for each genotype and age group. Horizontal and vertical OKR data were processed to extract gain values, where gain at each drum velocity was defined as the average slow-phase eye velocity divided by the drum/planetarium velocity. Plots of gain versus stimulus frequency (speed-tuning curves) were compiled for each recording session. As with the VOR/VVOR data, curves from at least two sessions were averaged to yield single-animal curves, and multiple single-animal curves were averaged to generate a curve for each genotype and age group. In descriptions of horizontal and vertical OKR results, positive drum rotations signify, respectively, temporal-nasal and upward rotations with respect to the recorded eye. Cross-axis adaptation data were processed to determine horizontal VOR gain, as well as vertical VOR gain defined as the amplitude of the vertical velocity divided by the amplitude of the *horizontal* stimulus. The progression of the horizontal and vertical gain changes through the adaptation period was compiled for each animal/age, and average curves from multiple animals were in turn averaged to generate a single curve for each age group.

In addition to the full-cycle Fourier analyses of VOR and VVOR gain described above, data were reanalyzed to determine whether there were differences in the gains of nasally and temporally directed eye movements. The analysis of each data sample (consisting of several cycles of stimulus and response at a single stimulus frequency) proceeded as follows: First, the multiple cycles were pointwise averaged to generate a single averaged cycle of stimulus and response. Second, Fourier analysis was used to fit the eye signal with a sinusoid. Third, the head and eye signals were each separated into two hemicycles, based on where the *fitted* eye velocities were positive or negative. Fourth, multiple linear regression was performed on the hemicycles of the eye and head movements, according to the regression equation $E(t)$ [or $H(t)$] $= A \sin 2\pi ft + B \cos 2\pi ft + C$, where A, B, and C are regression coefficients, f is stimulus frequency, and t is time. In the case of the nasally directed eye movement (and its associated oppositely directed hemicycle of head movement), t was restricted to those values where the fitted full-cycle eye velocity was positive. Conversely, for the temporally directed eye movement and the associated head movement, t was restricted to values for which the fitted full-cycle eye velocity was negative. Fifth, amplitudes of the eye ($|E|$) and head ($|H|$) for each hemicycle were determined from $\sqrt{(A^2 + B^2)}$, and gain was then quantified as $|E|/|H|$.

Responses to thrust stimuli were analyzed by determining, for each rotation, the direction of the ocular response in the plane of the video image, which was approximated as the arctangent of the ratio of the horizontal and vertical eye position changes from the beginning to the end of the head impulse. Response gain was calculated as the ratio of the radial change in eye position to the change in horizontal head position. The angles and gains from 10 to 30 impulses in each direction were then averaged to yield a pair of angles/gains for each animal/age.

Time constants (T) of the neural integrator were determined by fitting each centripetal drift with the exponential $E(t) = A \exp(-t/T) + C$, where t is time, E(t) is eye position, and A and C are fitting constants. We discarded epochs with duration <2.5 s, A <3°, or C >15° from the average equilibrium position, or if the generalized correlation coefficient ($r^2$) was <0.80. We calculated median time constants in each animal separately for abducting and adducting centripetal drifts and averaged across animals. Note that an "abducting centripetal drift" is a drift made from an initial adducted eccentric position.

All results are reported as means ± SD. Significance of interage group and intergenotype comparisons was tested as described in RESULTS. In general, curves were compared using repeated-measures ANOVA, whereas point measurements were compared using two-tailed *t*-test. Significance of differences in *x*-intercepts was assessed by *t*-test, making use of the intercept SE generated in the linear regression. Significance of regression analyses was tested using the *t*-test for $r^2$. Tests of regression significance were not corrected for multiple comparisons. Given the large number of parameters we desired to explore and practical limitations in the number of animals that could be tested, such correction would have generated an excessive risk of type II statistical error (the incorrect conclusion that a correlation is absent when, in fact, the two variables are related), thereby defeating the exploratory goals of the study. As usual, the reduction in the risk of type II statistical error is accomplished at the expense of an increased risk of the converse type I error (false conclusion that two variables are related), and thus the inferences regarding mechanisms drawn from the correlation analyses should be considered provisional in nature.

## RESULTS

### *Static elevation*

Figure 1 plots static pupil elevation in the light as a function of animal age. Regression lines have been superimposed. All three genotypes exhibited wide variations in elevation within any one age group, and there was extensive overlap between genotypes. Nevertheless, in *rocker* and *tottering*, elevations tended to be greater than that in controls. For *tottering*, the difference from controls was significant at $P < 0.001$ or better (two-tailed *t*-test) in all age groups, and the elevation trended upward with age (elevation vs. age $r^2 = 0.08$, $P = 0.114$, *t*-test for $r^2$). Elevations for *tottering* and controls averaged 25.6 ± 6.1° versus 17.8 ± 4.8°, 27.0 ± 3.2° versus 19.5 ± 4.8°, and 28.4 ± 5.1° versus 17.5 ± 3.2° in the young, middle, and old age groups, respectively. As already reported (Stahl 2004a), *rocker*'s elevation was initially normal, but increased significantly with age ($r^2 = 0.33$, $P = 0.002$), the group average becoming significantly different from controls ($P = 0.0014$) in the oldest age group. Human P/Q calcium channelopathies and other cerebellar disorders are frequently associated with downbeat nystagmus. However, as was the case in *rocker* (Stahl 2004a), *tottering* animals exhibited largely static (although elevated) vertical positions in light and darkness. In occasional animals downbeats followed by slow upward drifts did occur, particularly in the light. When present they were rare and irregular, rarely exceeding five beats in a 40-s record.

### *VOR/VVOR dynamics*

Figure 2 shows Bode plots for VOR and VVOR of controls and mutants in each age group. *Tottering* exhibited a similar pattern of gain abnormalities at all ages. The most prominent abnormality was the failure of VOR gain to increase with increasing stimulus frequency as rapidly as in controls, resulting in a large gain disparity at 1.6 Hz, although gain was subnormal at the low stimulus frequencies as well. VVOR gain was deficient at all frequencies. At the lowest frequencies, where VOR gain is closest to normal, the VVOR attenuation is attributed to a reduced optokinetic (visual) response, an attribution supported by the narrowing of the gap between the VVOR and VOR gain curves in *tottering* compared with controls. At the highest stimulus frequencies, the visual contribution to gain is normally small (note the small gap between VOR and VVOR gain curves in control animals), and thus *tottering*'s deficiency in VVOR gain at high stimulus frequencies is largely attributable to the subnormal VOR gain. The difference between gain values (both VOR and VVOR) of *tottering* and controls was significant at all frequencies and ages, usually at $P \leq 0.0001$. The lowest degrees of significance (highest *P* values) were obtained for 0.1 and 0.2 Hz in the dark in the youngest age group, in which the *P* values were 0.0046 and 0.0017, respectively. In contrast to *tottering*, *rocker* exhibited VOR gain abnormalities only at the highest stimulus frequencies. *Rocker*'s augmentation of gain in the presence of vision was normal in the youngest age group and only minimally impaired with aging, and thus VVOR gain curves in

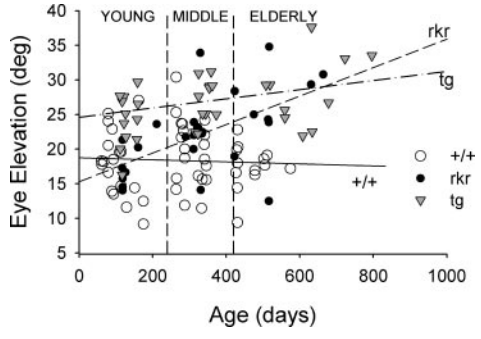


FIG. 1. Average vertical position of the eye in light plotted as a function of animal age. Each symbol represents a single animal. Dashed vertical lines represent the boundaries between the arbitrarily defined young, middle, and old age groups. Regression fits for control (solid line), *tottering* (dash–dot line), and *rocker* animals (dashed line) are superimposed. *Tottering* exhibited abnormal elevation at all ages.

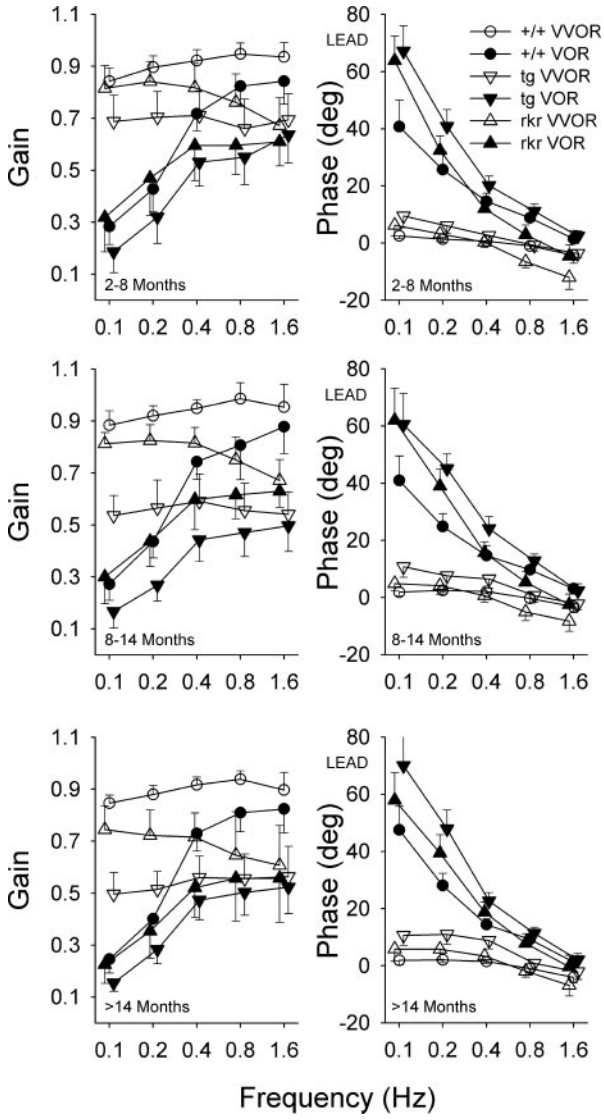


FIG. 2. Bode (phase and gain vs. stimulus frequency) plots for vestibuloocular reflex (VOR, filled symbols) and visually augmented vestibuloocular reflex (VVOR, open symbols) for mutants and controls. Data for young, middle, and old age groups are plotted separately. Data points are staggered horizontally and error bars (1 SD in length) are plotted unidirectionally for graphic clarity. *Tottering* mutants exhibited subnormal VOR and VVOR gains at all stimulus frequencies, whereas in *rocker* the attenuation was limited to higher stimulus frequencies. Both mutants strains also exhibited abnormally large VOR phase leads at low stimulus frequencies.

*rocker* exhibited prominent declines with increasing stimulus frequency, merging with the *tottering* gain curves at 1.6 Hz.

Phase curves were also mildly abnormal in *tottering*. At all ages, VOR phase led controls at the lowest stimulus frequencies. At 0.1 Hz the disparities between the average curves were 26.4 ± 7.0, 19.6 ± 8.2, and 22.5 ± 8.4° in the early, middle, and late age groups, respectively (values are the 95% confidence intervals for differences between means of independent samples). The *tottering* and control VOR phase curves gradually merged with increasing frequency. At each age the difference between VOR phase in *tottering* and controls was significant at $P \leq 0.0001$ for stimulus frequencies of ≤0.4 Hz, and $P < 0.05$ or better at 0.8 Hz. VVOR phase curves also exhibited a consistent tendency for *tottering* to lead controls at the lowest frequencies, which could be explained by an inability of *tottering*'s weakened optokinetic response to compensate fully for the excessive lead of the vestibular response. *Rocker* also exhibited abnormally large phase leads during 0.1- and 0.2-Hz VOR and VVOR, the values being intermediate to those of *tottering* and controls.

To generate insight into whether the abnormalities of VOR/VVOR dynamics described above were congenital or acquired, we regressed the most abnormal parameters versus animal age. (Of note, the conclusion that any feature is "congenital" is a provisional one; see DISCUSSION.) Scatterplots of VOR and VVOR gains versus age are shown in Fig. 3. In *tottering*, VOR gain at 1.6 Hz declined slightly with age [linear regression slope (m) = $-1.9 \times 10^{-4}$ day$^{-1}$, $r^2 = 0.12$, $P = 0.049$], but most of the subnormality may still be congenital because the regression lines of mutants and controls were so nearly parallel and so widely separated that they did not converge when extrapolated backward to birth (*y*-intercepts differ significantly, $P < 0.0001$). Likewise, the gain deficit at 0.1 Hz may be congenital, as the regression curve failed to reach significance ($P = 0.32$) and roughly paralleled the control curve (*y*-intercepts differ, $P = 0.0005$). The VVOR gain of *tottering* at 0.1 and 1.6 Hz declined gradually with age and, unlike the case for VOR gains, the correlation coefficients were statistically significant (at 0.1 Hz: m = $-3.5 \times 10^{-4}$ day$^{-1}$, $r^2 = 0.36$, $P < 0.001$; at 1.6 Hz: m = $-2.4 \times 10^{-4}$ day$^{-1}$, $r^2 = 0.17$, $P = 0.015$). Again, the *y*-intercepts for *tottering* and control VVOR gains differed significantly for 0.1 Hz ($P = 0.0004$) and 1.6 Hz ($P < 0.00001$). However, the regression lines for *tottering* and control gains at 0.1 Hz did converge to within 0.15 at the *y*-intercept, whereas the regression lines for 1.6 Hz were closer to parallel, and were still separated by a gain of 0.27 at the *y*-intercept. These results suggest that the VVOR gain deficit exhibits both acquired and congenital components at both frequencies, but the acquired component dominates at low frequencies and the congenital component is more pronounced at high frequencies. These differences in the VVOR gain versus age relationships at different stimulus frequencies are consistent with the differing visual and vestibular contributions to the response at each frequency, the magnitude of the mutation-related VOR gain deficits, and the age-related decline in optokinetic performance described below. Specifically, at 1.6 Hz there is a large initial VOR gain deficit that increases only slightly with age, and a minimal optokinetic contribution to VVOR gain, and thus despite the tendency of OKR to diminish through life, the VVOR gain deficit at 1.6 Hz is initially large and progresses minimally. Conversely, at 0.1 Hz the VOR gain deficit is small and largely age independent, whereas the optokinetic contribution to the VVOR is large. Thus the VVOR gain deficit at 0.1 Hz is initially small, but increases with age in step with the OKR. The other consistent difference between the dynamics of *tottering* and control animals was the mutant's larger VOR phase lead at the 0.1-Hz stimulus frequency. Both *tottering* and control exhibited trends toward increasing 0.1-Hz phase lead with age, but the correlation coefficients were low and statistically nonsignificant ($r^2 = 0.01$, $P = 0.58$ and $r^2 = 0.06$, $P = 0.11$), consistent with the larger phase lead in *tottering* reflecting a congenital defect.

### *Neural integrator function*

The increased phase lead at low stimulus frequencies could be explained by an abnormally short time constant of the brain stem neural integrator, which synthesizes the tonic command signals required to compensate for the elasticity of the ocular motor plant (Skavenski and Robinson 1973), and as such is responsible for much of the required phase lag between the

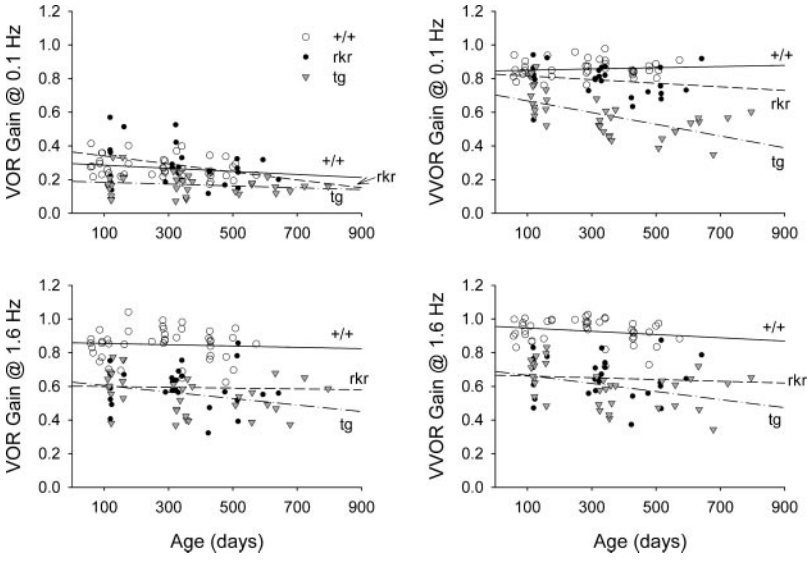


FIG. 3. Scatterplots of VOR and VVOR gains vs. animal age. Each symbol represents a single animal. Regression fits for control (solid line), *tottering* (dash–dot line), and *rocker* animals (dashed line) are superimposed.

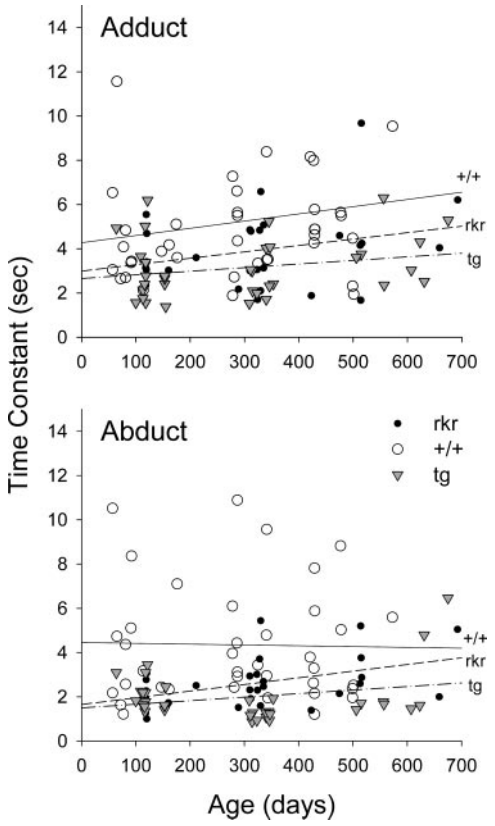


FIG. 4. Time constant of the neural integrator plotted as a function of animal age. Each symbol represents a single animal. Regression fits for control (solid line), *tottering* (dash–dot line), and *rocker* animals (dashed line) are superimposed. "Abduct" and "adduct" refer to the direction of the drift (opposite the direction of initial eye displacement). Both mutant strains exhibited reduced time constants (poorer gaze stability in darkness) in comparison to controls, particularly for abducting drifts.

modulation of primary vestibular afferents and motoneurons. Neural integrator time constants were determined in control, *tottering*, and *rocker* animals by fitting single-exponential decays to the centripetal drifts that occurred when the lights were extinguished after bringing the eye to an eccentric position. Figure 4 shows the time constants for abducting and adducting centripetal drifts, plotted versus animal age. Linear regression on the data for all three strains suggested a weak tendency for time constants to increase with age, but the interanimal variability was wide, and the only regression that was significant at $P < 0.05$ or better was that of the abducting drifts in *rocker* ($r^2 = 0.19$, $P = 0.024$). Because the regression lines of mutants approximately paralleled controls, the deficient integrator time constant may be provisionally considered a congenital abnormality. Averaging animals of all ages, adducting and abducting time constants were 5.2 ± 3.1 and 4.5 ± 2.5 s for controls, 3.2 ± 1.3 and 2.0 ± 1.1 s for *tottering*, and 3.9 ± 1.8 and 2.6 ± 1.2 s for *rocker*. *Tottering* differed from controls at $P < 0.001$ or better, and *rocker* differed from controls at $P = 0.001$ for abducting and $P = 0.065$ for adducting drifts. Assuming that the neural integrator can be modeled as a one-pole lag element whose time constant is the average of our measured abducting and adducting values, the shorter time constants of *tottering* and *rocker* would translate to an increase in phase lead (decrease in lag imparted by the integrator) with respect to controls of 13.3° for *tottering* and 7.9° for *rocker*, at a stimulus frequency of 0.1 Hz. The actual differences obtained from the VOR data of all animals were 23.0 and 18.2°, indicating that our measures of integrator dysfunction can explain approximately half of the increased phase lead of the mutant strains.

### *OKR speed tuning*

Figure 5 depicts horizontal OKR speed-tuning curves for each of the three age groups. *Tottering* exhibited mild reductions in horizontal OKR gain, and the *tottering* and control tuning curves differed significantly by repeated-measures ANOVA for all three age groups ($P = 0.011$, $P < 0.001$, $P < 0.001$, respectively). The deficit was most pronounced at the lowest drum speeds and for the temporal-nasal direction of drum rotation. *Rocker* OKR gains tended to be intermediate between those of controls and *tottering* and, in fact, the *rocker* curve became significantly different from control only in the oldest age group (Stahl 2004a). Inspection of the speed-tuning curves in Fig. 5 suggests the possibility of a combination of congenital and acquired deficits in OKR gain in *tottering*. We investigated this possibility by regressing OKR gains versus animal age, concentrating on the responses to 10°/s rotation, the speed at which the disparity between *tottering* and control gains was particularly pronounced. Figure 6 shows the gain versus age plots for 10°/s rotation in the nasal-temporal and temporal-nasal directions. Regression fits for control animals were flat, indicating that OKR gain is normally stable over a broad range of animal age. The *y*-intercepts of the *tottering* curves were significantly lower than those of control for both nasal-temporal ($P = 0.03$) and temporal-nasal ($P = 0.0018$)

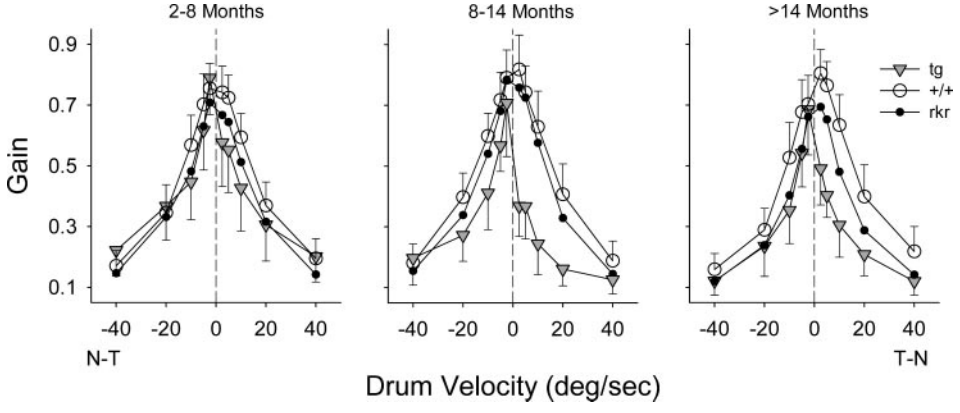


FIG. 5. Plots of horizontal optokinetic response (OKR) gain vs. stimulus velocity for mutants and controls. Data for young, middle, and old age groups are plotted separately. *Rocker* data are reproduced from previous study (Stahl 2004a) and error bars are suppressed for graphic clarity. Other error bars are 1 SD and plotted unidirectionally for clarity. Dashed line marks 0°/s. N-T: nasal-temporal; T-N: temporal-nasal. With age, *tottering* gain became progressively subnormal and the divergence from the symmetry of control gains became more pronounced.

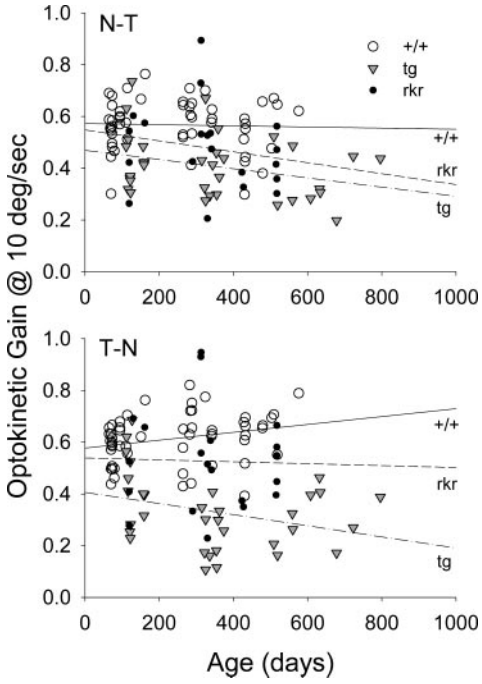


FIG. 6. Gain of the horizontal OKR for 10°/s rotations of the optokinetic drum, plotted vs. animal age. Results are plotted separately for nasally and temporally directed drum rotations with respect to the recorded eye (indicated on the plots as "T-N" and "N-T"). Each symbol represents a single animal. Regression fits for control (solid line), *tottering* (dash–dot line), and *rocker* animals (dashed line) are superimposed. Both mutant strains diverged from controls with increasing age.

directions, consistent with a congenital gain deficit. The intercepts were also significantly lower for temporal-nasal rotations at 2.5°/s ($P = 0.0012$) and 5°/s ($P = 0.0012$) (plots not shown). The gain versus age plots also suggested an acquired component to the gain deficit because gains trended downward for both directions of rotation at 2.5, 5, and 10°/s. None of these trends reached statistical significance. For 10°/s, the correlation coefficients and associated $P$ values were $r^2 = 0.09$ ($P = 0.078$) for nasal-temporal rotation and $r^2 = 0.10$ ($P = 0.065$) for temporal-nasal rotation. Regression significance would certainly have been depressed by the large interanimal variability. The possibility that the downward trend is meaningful despite the statistical nonsignificance is supported by two observations. First, OKR gains clearly declined with age in *rocker* (Stahl 2004a). Assuming that allelic mutant strains share abnormal features, the clear age-related decline in *rocker* makes it more likely that the decline in *tottering*, although shallow, still reflects a true relationship between gain and age. Second, an acquired decline in OKR gain of Cacna1a mutants would explain the observation that the low-frequency VVOR gains of *tottering* and *rocker* diverge from control values with increasing animal age (see above).

*Tottering* horizontal OKR speed-tuning curves exhibited a striking asymmetry, with gain being lower during temporal-nasal rotation of the drum with respect to the recorded eye. To determine whether this asymmetry is specific to visually driven eye movements, we reanalyzed the VVOR and VOR data of the middle- and older-aged animals (the groups in which temporal-nasal gains diverged most strikingly from controls) to determine whether gains differed for the nasally and temporally directed hemicycles of eye rotation. These hemicycle gains are plotted along with similar data for control animals of all ages in Fig. 7. The figure demonstrates that in both *tottering* and controls, VOR and VVOR gains were slightly greater during the nasally directed hemicycle, similar to the asymmetry described for VOR in the normal gerbil (Kaufman 2002). *Tottering*'s VOR and VVOR gain asymmetries were therefore similar to those of normal animals, but opposite to those observed during their constant velocity OKR. The magnitudes of the gain disparities tended to be similar in VOR and VVOR, particularly for control animals (note, for instance, how the curves approach each other at 0.1 and 0.8 Hz in both VOR and VVOR), which could indicate that the mechanism responsible for the gain asymmetry is located at a point after optokinetic and vestibular signals have become combined within the same neurons, or that it lies within the VOR pathway, and the optokinetic system entirely fails to compensate for the asymmetry.

Of note, the fact that the gain asymmetry observed in *tottering* OKR did not confer a similarly directed asymmetry on its VVOR (or, at least, lessen the degree by which their nasally directed VVOR gain exceeded temporally directed gain) was somewhat surprising. One possible explanation is that nasally directed OKR gain was diminished only because the mutants failed to sustain eye velocity throughout the entire 4-s duration of each constant velocity stimulus. In this case the asymmetry would appear in the OKR, but not in the responses to the oscillatory VVOR stimuli. We tested this possibility by comparing optokinetic gains calculated from the entire constant velocity period to gains determined from only the first half (2 s) of the period. We focused on the nasally directed OKR at 2.5–10°/s in the pooled 8- to 14-mo and >14-mo mutants ($n = 21$ animals), the conditions and ages in which temporal-nasal gains diverged most strikingly from controls. These initial and overall gains proved to be equivalent, averaging, respectively, 0.42 ± 0.15 versus 0.43 ± 0.12 at 2.5°/s ($P = 0.71$, paired $t$-test), 0.40 ± 0.14 versus 0.38 ± 0.09 at 5°/s ($P = 0.34$), and 0.28 ± 0.11 versus 0.27 ± 0.11 at 10°/s ($P = 0.56$). Thus the OKR asymmetry does not arise from an inability to sustain the response to the constant velocity temporal-nasal optokinetic stimulus.

The most straightforward interpretation of the horizontal OKR speed-tuning curve is that the sensitivity to optokinetic stimulation is reduced, and more so for the temporal-nasal

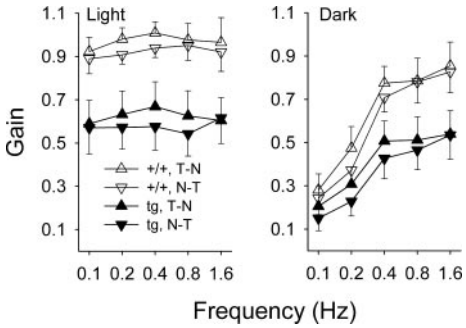


FIG. 7. Average hemicycle gains for *tottering* (8- to 14-mo and >14-mo age groups, only) and control animals, plotted as functions of stimulus frequency. A slight increase in the gain of nasally directed ("T-N") compared with temporally directed ("N-T") eye movements is present in both VOR and VVOR in mutants and controls. Note that the gain asymmetry in *tottering* is opposite to that seen in its optokinetic speed-tuning curves (Fig. 4). Error bars are 1 SD and plotted unidirectionally for clarity.

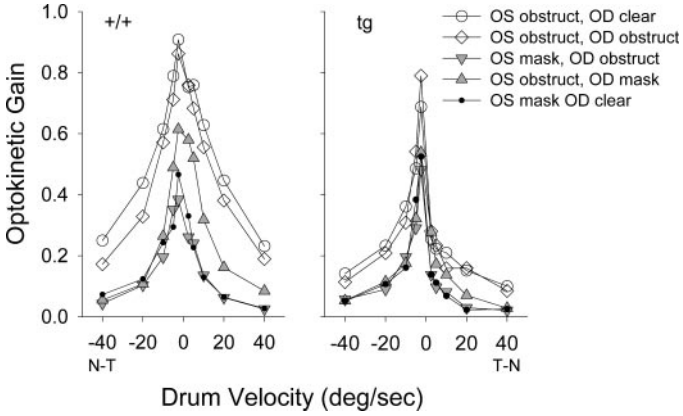


FIG. 8. Effect of various asymmetrical visual stimulation conditions on horizontal OKR speed tuning in 4 young control animals (*left*) and 5 middle-aged *tottering* mutants (*right*). All eye movements were recorded from left eye. OS, left eye; OD, right eye. Clear: indicated eye has completely unobstructed view of optokinetic drum. Obstruct: view partially obstructed by actual or mock oculography apparatus. Mask: view fully obstructed by a cloth drape. "OS obstruct, OD clear" condition (or its converse, when recording from the right eye) corresponds to the usual recording arrangement in this study.

direction of drum rotation. However, a complication is introduced by the fact that the optokinetic stimulation delivered to each eye was not perfectly matched; the recorded eye's view of the optokinetic drum was mildly obstructed by the presence of animal-fixed apparatus (the camera and infrared illuminators) in the foreground. If the OKR in mutants were driven to an extent greater than that in controls by the eye receiving temporal-nasal stimulation, then the asymmetry in optokinetic stimulation would reduce mutant OKR gain during temporal-nasal rotation. We explored this possibility by manipulating the optokinetic stimulation to each eye in a subgroup of five middle-aged mutants and four young controls. For the purposes of the following description, "obstruction" refers to a partial obstruction of the view of the optokinetic drum by animal-fixed apparatus. In the case of the recorded eye, the obstruction was generated by the camera and illuminators. In the case of the opposite eye, the obstruction was generated by a dummy copy of the recording apparatus that was positioned to approximate the visual effects of the actual recording apparatus. The "mask" was a gray cloth drape that could be positioned on either side of the turntable to entirely block the view of the drum on one side. In the case of the recorded eye, the mask was perforce placed outside the recording apparatus. Figure 8 shows average speed-tuning curves for controls and *tottering*. As in the tuning curves generated from the larger sample (see Fig. 5), the mutants evinced attenuated and asymmetrical gains. In controls, adding the obstruction to the contralateral, nonrecorded eye (i.e., balancing the optokinetic stimuli) generated a mild reduction in gain for both nasally and temporally directed eye movements. Masking the nonrecorded eye moderately reduced gains in both directions, slightly more so for temporally directed eye movements. This result is consistent with the possibility that the ability of the contralateral eye to drive the ipsilateral eye is greater for temporal-nasal than nasal-temporal stimulation (re the contralateral eye).

However, the temporal-nasal movement of the ipsilateral eye is still driven predominantly by the ipsilateral visual stimulation because masking the ipsilateral eye produced the largest gain attenuation for both directions of movement, and adding an additional obstruction to the contralateral eye had little additional effect. In the case of *tottering*, the speed-tuning curves for all conditions were attenuated and the disparities were compressed. Nevertheless, the same rank order was observed. Balancing the obstruction had minimal effects and, significantly, failed to correct the asymmetry. Masking the contralateral eye had intermediate effects. Masking the ipsilateral eye had the most severe effects and the addition of obstruction to the contralateral eye was largely irrelevant. Notably, masking the contralateral eye did not result in a more severe attenuation of temporally than nasally directed eye movements, as would have been the case if *tottering* eye movements were driven primarily from whichever eye received temporal-nasal stimulation. Thus the results are consistent with a reduction of movement of the eye receiving temporal-nasal optokinetic stimulation, rather than a reduction in motion of both eyes, resulting from a larger dependency on temporal-nasal stimulation interacting with our mildly asymmetrical optokinetic stimulus.

OKR speed tuning was also assessed for optokinetic stimulation about the roll axis, as a response to roll visual motion is a prerequisite for the ability to undergo cross-axis adaptation tested below. (It should be noted that the two-dimensional [2D] oculography provides only an approximation of the actual response because the stimulus and response axes are rotated approximately 45° to the optical axis of the camera. In contrast, the horizontal gain measurements are more accurate because the stimulus/response axis and the camera's optical axis are perpendicular.) The roll (vertical) OKR speed-tuning curves are shown in Fig. 9. Control data were collected from only the youngest and oldest age groups, but the tuning curves were similar at those two ages ($P = 0.39$, repeated-measures

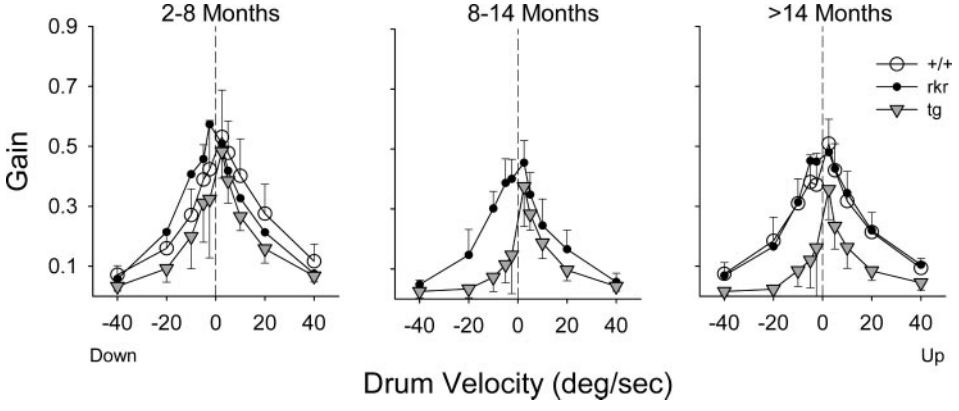


FIG. 9. Plots of vertical OKR gain vs. stimulus velocity for mutants and controls. Data for young, middle, and old age groups are plotted separately. Error bars are 1 SD and plotted unidirectionally. Dashed line marks 0°/s. *Rocker* error bars in the youngest and oldest age groups are suppressed for graphic clarity. *Tottering* vertical OKR gains declined with age, particularly for downward rotation of the planetarium with respect to the recorded eye.

ANOVA), indicating that the vertical optokinetic response, like the horizontal optokinetic response, is normally stable through life. *Tottering* of the youngest age group exhibited mildly, but significantly, reduced gains compared with those in controls (repeated-measures ANOVA, $P = 0.006$). With increasing age, the response declined, particularly during downward optokinetic stimulation. Regressing gain versus age for 10°/s rotations yielded correlation coefficients and associated $P$ values of $r^2 = 0.24$ ($P = 0.0054$) for downward rotation and $r^2 = 0.33$ ($P = 0.0007$) for upward rotation, consistent with the acquired (or at least, progressive) nature of the vertical gain deficit in this strain. Gain versus age plots were also negatively sloped for both directions at 2.5°/s (down: $r^2 = 0.09$, $P = 0.10$; up: $r^2 = 0.15$, $P = 0.03$) and 5°/s (down: $r^2 = 0.32$, $P = 0.001$; up: $r^2 = 0.41$, $P = 0.0001$). Average vertical OKR gains for young *rockers* varied around the curve for the control animals ($P = 0.74$, repeated-measures ANOVA), and in the oldest age group the *rocker* and control curves overlapped extensively (ANOVA, $P = 0.68$). Because of the decline in vertical OKR in *tottering*, analysis of the cross-axis data from this strain was restricted to the youngest age group (see following text). The relative stability of the vertical OKR in *rocker* and controls supports the decision to pool animals of all ages in the analysis of the cross-axis data in this and the previous study (Stahl 2004a). Furthermore, the mild degree of reduction in *rocker*'s vertical OKR argues against attributing its lifelong deficiency in cross-axis adaptation (Stahl 2004a) to an inability to respond to the adapting stimulus.

### *Correspondence of VOR stimulus and response axes*

Ideally, the axis of a compensatory eye movement should align perfectly with the axis of the vestibular or visual stimulus. However, VOR stimulus–response misalignments are exhibited by humans with cerebellar disorders and form the basis of a bedside test in which the clinician observes aberrant vertical eye movements elicited by small-amplitude, brisk horizontal head rotations (so-called thrusts) (Walker and Zee 1999). Mice were tested using analogous brisk, low-amplitude rotations in the light, and the 2D response angle and gain were determined from the changes in eye position. The effects of age on angle and gain were assessed by linear regression. There was no significant effect of age on either parameter for *rocker* and control (regression $P \geq 0.23$), or for the angle of *tottering*'s abducting eye movements. The correlation was significant for the angle of *tottering*'s adducting eye movements, but the slope was shallow (slope $= -0.006°\ \text{day}^{-1}$, $r^2 = 0.11$, $P = 0.049$). More notable was *tottering*'s significant decline in gain with age for both abducting (slope $= -2.2 \times 10^{-4}\ \text{day}^{-1}$, $r^2 = 0.15$, $P = 0.021$) and adducting movements (slope $= -2.5 \times 10^{-4}$, $r^2 = 0.20$, $P < 0.001$), which accords with this strain's slight but significant decline in VOR gain at 1.6 Hz described above. Because the effects of aging on angle were absent or slight, we pooled animals of all ages and plotted the angles and gains in polar format in Fig. 10. Abducting eye movements are plotted to the left and adducting movements to the right. Normal animals exhibited a moderate misalignment, such that, on average, the eye tended to move downward during adduction and upward during abduction. The magnitude of the deviation from the ideal trajectory was small: 2.4 ± 2.6 and 3.4 ± 2.4° for adducting and abducting movements,

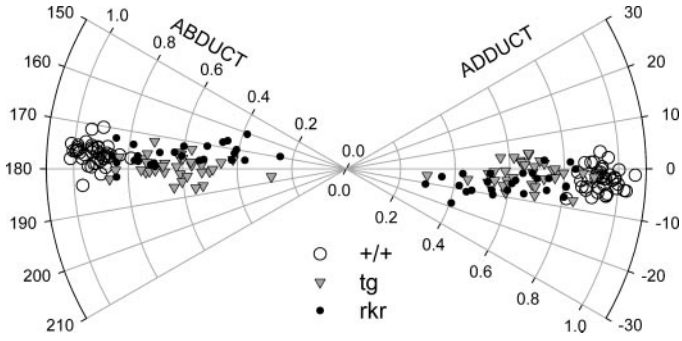


FIG. 10. Polar plot summarizing results of thrust experiment, which were assessed for concordance of VOR response and stimulus axes. Gain of eye movement is plotted vs. angle of movement, as projected onto the plane of the video image. Each plotting symbol represents data from one animal. Small degrees of misalignment were demonstrated in control and *rocker*, but not *tottering*, strains.

respectively. The error is unlikely to be related to a misalignment of the camera roll axis because this adjustment was carefully verified (see METHODS). Moreover, we recorded variously from the right or left eye; if the camera axis had been tilted, the apparent VOR misalignments would have been opposite for the two eyes. *Rocker* and *tottering* mutants tended to exhibit lower-amplitude responses, in keeping with their lower high-frequency VOR gains described above. *Rocker* mutants whose gains most closely approximated control animals exhibited misalignments that, likewise, approached those of the controls. Decreasing gain was associated with an increasing degree of misalignment. The averages of the *tottering* responses, in contrast, were centered on the stimulus axes, and this alignment appeared to be preserved irrespective of gain. Response angles for *rocker* differed from control for both abduction ($P = 0.009$, one-way ANOVA with genotype as factor) and adduction ($P = 0.001$). *Tottering* differed from control for abduction ($P = 0.001$) but not adduction ($P = 0.438$).

### *Cross-axis adaptation*

Figure 11 displays the progress of gain changes for rotation in the light (response to the adaptation stimulus) and dark during the course of the 50-min cross-axis adaptation period. Control and *rocker* curves, reproduced from the previous study, were created by pooling animals of all ages (Stahl 2004a). In contrast, the *tottering* curves are based exclusively on data drawn from the 12 animals in the youngest age group because older animals developed a considerable reduction in response to the roll optokinetic stimulus, increasing the possibility that deficiencies in cross-axis adaptation reflect an inability to respond to the adapting stimulus. Despite young *tottering*'s ability to generate a response to the roll optokinetic stimulus (see above), there was no appreciable vertical response at any time during the cross-axis paradigm. The result contrasted markedly with that of *rocker*, which, as a group, exhibited a detectable vertical response at first exposure to the adapting stimulus, a mild (although subnormal) increase in that light response over the course of the adaptation period, and a slight but detectable increase in vertical motion in darkness by the end of the experiment. *Rocker*'s deficient but detectable vertical responses were enhanced by adjusting for its decline in *horizontal* VOR gain across the adaptation period (Stahl

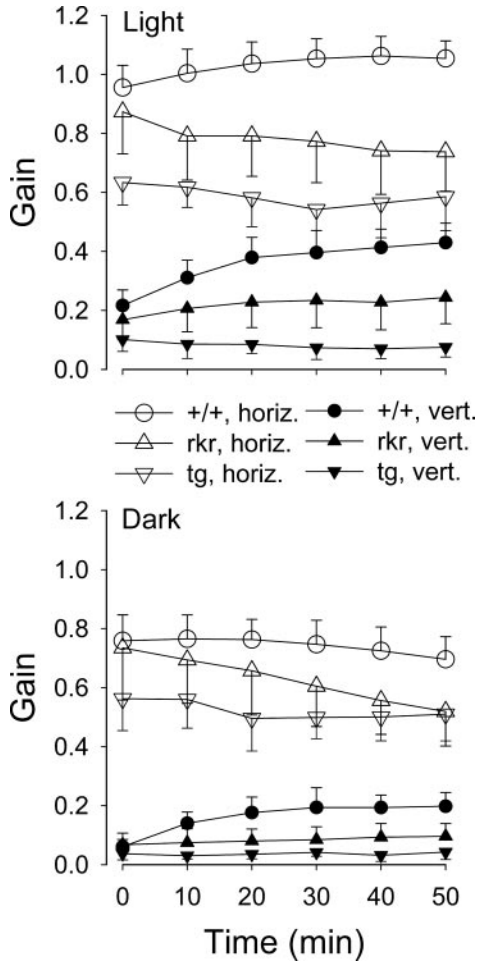


FIG. 11. Alteration of horizontal and vertical gains in light (*top*) and darkness (*bottom*) over the course of the 50-min cross-axis adaptation experiment. *Tottering* data restricted to the 2- to 8-mo age group, whereas control and *rocker* data pools animals of all ages. Vertical and horizontal gains are plotted as filled and open symbols, respectively. "Light" gains are obtained in the presence of the adapting optokinetic stimulus. All error bars are 1 SD and are plotted unidirectionally for graphic clarity. *Tottering* failed to develop cross-coupled vertical movements in darkness, whereas *rocker* demonstrated some ability to augment its vertical movements to the adapting stimulus.

2004a). In contrast, Fig. 11 demonstrates that *tottering*'s horizontal responses in light and dark were quite stable and thus there was no reason to speculate that a developing vertical response was being masked by habituation of the entire vestibular system. Correcting vertical gain in the style of the previous study (plots not shown) succeeded only in emphasizing the contrast between *rocker*'s minimal preservation and *tottering*'s absolute lack of cross-axis adaptation.

The initial (preadaptation) amplitude of the vertical eye movement elicited by the adaptation stimulus differed significantly in the three strains, with the rank order: control > *rocker* > *tottering* (*rocker* vs. control, $P = 0.0071$; *tottering* vs. control, $P < 0.0001$, *t*-test). The averaged capacity to adapt followed the same rank order, raising the possibility that interstrain and animal-to-animal variations in the degree of adaptation are actually attributable to variations in the ability to respond to the adaptation stimulus. We tested this possibility by regressing the change in vertical gain (defined as the average of vertical gains in the dark at 30 and 40 min minus the preadaptation gain in the dark) versus the preadaptation vertical gain in the light. The correlations (plots not shown) were flat and none of the slopes was significantly different from zero (control: $r^2 = 0.00$, $P = 0.95$; *rocker*: $r^2 = 0.01$, $P = 0.66$; *tottering*: $r^2 = 0.02$, $P = 0.57$). Analogous plots of the change in vertical gain in the light versus initial vertical response actually exhibited negative slopes (lower initial response associated with larger change in gain) for all strains. Thus variations in the degree of adaptation are not simply a reflection of variations in the magnitude of the vertical eye movement induced by the adaptation stimulus.

### *Fast phase dynamics*

As was the case for *rocker* and C57BL/6 controls (Stahl 2004a), *tottering* exhibited a strong linear relationship between fast phase peak velocity and amplitude, and abducting fast phases tended to be slower than adducting fast phases. Averaging *tottering* animals of all ages, these abduction and adduction velocity–amplitude slopes were respectively 22.2 ± 1.2 and 25.3 ± 1.4 $s^{-1}$, and the difference was statistically significant (paired *t*-test, $n = 31$, $P < 0.0001$). Figure 12 plots the slopes for mutants and controls versus age for the abducting (*top*) and adducting (*bottom*) directions. For all genotypes, velocity–amplitude slopes for adducting fast phases were stable through life ($r^2 \leq 0.04$, $P \geq 0.17$). For abducting fast phases, there was a moderate decline in both *tottering* (−0.0024 $s^{-1}$ $day^{-1}$, $r^2 = 0.18$, $P = 0.016$) and *rocker* (−0.0036 $s^{-1}$ $day^{-1}$, $r^2 = 0.12$, $P = 0.089$), which contrasted with the slight increase in slopes for controls (+0.0025 $s^{-1}$ $day^{-1}$, $r^2 = 0.08$, $P = 0.035$). Considering only the youngest age group, velocity–amplitude slopes were very similar for *tottering* versus controls for both abducting (22.9 ± 0.89 vs.

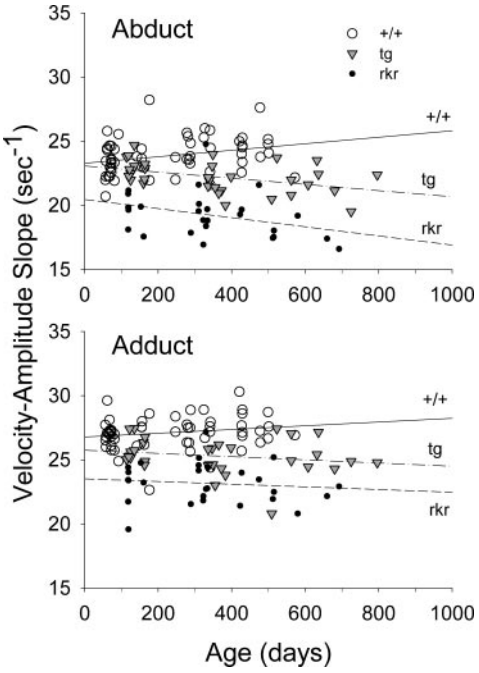


FIG. 12. Slopes of velocity–amplitude relationships for nystagmus fast phases plotted vs. animal age. Abducting and adducting fast phases are plotted separately. Each symbol represents data from one animal. Regression fits for control (solid line), *tottering* (dash–dot line), and *rocker* animals (dashed line) are superimposed. Slopes were initially normal in young *tottering*, but moderately declined with age. *Rocker* fast phases were slowed at all ages.

23.5 ± 1.5, $P = 0.18$) and adducting (25.8 ± 0.97 vs. 26.9 ± 1.2, $P = 0.012$) fast phases. Because of the divergent slope versus age relationships, *tottering* fast phases of both directions became considerably slower than controls in the middle and older age groups (all comparisons, $P \leq 0.001$). In contrast, *rocker* fast phases of both directions were significantly slower than controls in all age groups ($P \leq 0.001$) and slower than *tottering* ($P \leq 0.01$) in all age groups, except for the case of adduction at 8–14 mo, where significance reached only $P = 0.075$.

It should be noted that all the velocity–amplitude slopes reported here are underestimated as a result of the necessity of low-pass filtering the eye position traces before calculating eye velocity. To provide some insight into the degree of underestimation, we reanalyzed fast phases from the five control animals in which data were acquired with the higher video sampling rate (240 Hz). The higher sampling rate supported a commensurately higher analysis cutoff frequency (80 rather than 40 Hz). Velocity–amplitude slopes for 40- and 80-Hz cutoff frequencies averaged 23.6 versus 30.6 $s^{-1}$ and 27.1 versus 39.7 $s^{-1}$ for abducting and adducting fast phases, respectively. The underestimation is appreciable, but would be expected to act as a ceiling effect, disproportionately slowing the most rapid fast phases and thereby compressing any differences between genotypes. As such, the underestimation does not invalidate the conclusion that older *tottering* and all *rocker* mutants exhibit slower fast phases compared with controls.

### *Relationship of performance measures*

For many of the ocular motor indices quantified above, the degree of abnormality varied across animals of one mutant strain. If these variations originate from a common source (such as a variable degree in the reduction of dendritic calcium currents), then one might expect the variations in behavior to be correlated. For instance, an animal with a particularly depressed OKR gain might also have a more depressed VOR gain. This prediction was assessed in the previous study of *rocker* and control animals (Stahl 2004a), and linkages were demonstrated between static elevation and other abnormalities, and between VOR phase lead at 0.2 Hz and VOR gain at 1.6 Hz. Similar pairwise linear regressions were conducted between the most striking (but also variable) abnormalities of *tottering*'s ocular motor behavior (i.e., static elevation), VOR gain at 1.6 Hz, VOR phase at 0.1 Hz, average of abducting and adducting neural integrator time constants, *absolute* nasal-temporal ("N-T") OKR gains at 10°/s, *ratio* of T-N and N-T OKR gains at 10°/s, *absolute* upward OKR gains at 10°/s, and *ratio* of downward:upward OKR gains at 10°/s. Note that in the case of the OKR data, it was necessary to test correlations only with the T-N:N-T ratio and one of the absolute gains because testing correlations with the ratio and *both* absolute gains would be redundant. Based on our analysis of the OKR asymmetries above, the N-T absolute gain reflects the best performance of *tottering*'s optokinetic system, whereas the T-N:N-T ratio captures the asymmetry. For similar reasons, we assessed only the upward gain of the vertical OKR and its downward:upward ratio. It should also be noted that, although the complete lack of cross-axis plasticity was a strong abnormality, it was also invariant, and thus inappropriate for an investigation of the covariation of abnormal features. In the discussion below, correlation coefficients ($r^2$) are signed according to the sign of the regression slope to facilitate recognizing the sense of the relationships. As discussed in METHODS, significance tests were not corrected for multiple comparisons, so the results must be considered provisional in nature.

In control animals, only two of the pairwise correlations were significant at $P < 0.05$. Greater N-T OKR gain was associated with a smaller T-N:N-T ratio, and greater upward OKR gain associated with a smaller down:up OKR gain ratio. Both of these relationships are expected (in each case a larger value of the absolute gain in the denominator results in a lower gain ratio), provided that sources of variability of the pairs of absolute OKR gains (i.e., downward and upward, or T-N and N-T) are independent.

In *tottering*, there were four significant correlations. Greater ocular elevation was associated with reduction of the down:up OKR gain (signed $r^2 = -0.311$). Although this result raises the possibility that an imbalance in vertical optokinetic tone causes the greater static elevations, *rocker* did not exhibit the same relationship, despite sharing the static elevation abnormality (signed $r^2 = +0.17$, $P = 0.18$). The second significant association in *tottering* was between the T-N:N-T and down:up OKR ratios (signed $r^2 = +0.289$), suggesting a connection between the OKR asymmetries in different axes. Finally, both N-T and upward OKR gains were positively associated with VOR gain at 1.6 Hz (respective $r^2$ values of +0.186 and +0.249), indicating that animals exhibiting poorer OKR gains were more likely to be impaired in their VOR gain as well. Although the corresponding regression analyses in *rocker* did not reach significance, the regression slopes had the same sign (N-T OKR gain vs. VOR gain $r^2 = +0.151$, $P = 0.051$; upward OKR gain vs. VOR gain $r^2 = +0.241$, $P = 0.11$). Thus a similar relationship between OKR and VOR gains could be present in this mutant. It may be masked in part by the smaller number of *rocker* animals. One correlation that might have been predicted was absent (i.e., an association between shorter integrator time constants and larger VOR phase leads at low stimulus frequencies). An explanation for this nonassociation as well as implications of the correlations for underlying pathophysiological mechanisms are addressed in the DISCUSSION.

## DISCUSSION

*Tottering* mutants exhibited a broad range of abnormalities in compensatory eye movements and associated aspects of ocular motility. In most instances these abnormalities were quantitatively more severe than those observed in *rocker*, another Cacna1a mutant, just as the defects of gross motor coordination (ataxia) in *tottering* are more severe than those in *rocker*. Normal ocular motility reflects the synergy of multiple subsystems (Leigh and Zee 1999) and the ocular motor abnormalities could stem from dysfunction within different circuits, or from dysfunction within a particular circuit shared by the different subsystems. Below, we discuss the abnormalities individually and then proceed to assess how comparisons between different abnormalities, and between variations with animal age and mutant strain, allow us to generate hypotheses regarding the source (or sources) of ocular motor dysfunction.

*Static elevation*

*Tottering* mutants exhibited an upward deviation of eye position at rest and this hyperdeviation trended upward with aging. This result differed slightly from the case of *rocker*, in which the hyperdeviation appeared only with aging and thus was argued to represent an acquired abnormality, possibly stemming from degenerative effects of the mutation rather than from a direct effect of altered calcium current on neuronal signal processing (Stahl 2004a). Because the regression of *tottering*'s vertical position versus age had a positive slope (albeit one that missed statistical significance), it is conceivable that in this strain, too, the effect is acquired, but the process initially progresses so rapidly that the hyperdeviation is already present at the earliest age we recorded. Alternatively, the demonstrated abnormalities could reflect a mixture of congenital and acquired mechanisms. To date, we have observed the hyperdeviation in every ataxic mutant we have studied, including Cacna1a mutants *rocker*, *tottering*, and *tottering-4J* (unpublished results), as well as *lurcher* (Stahl 2002), an unrelated mutant that suffers complete degeneration of the cerebellar cortex (Caddy and Biscoe 1976; Zuo et al. 1997). We have speculated (Stahl 2004a) that the abnormality could be the murine homologue of downbeat nystagmus (DBN) found in humans carrying CACNA1A mutations, originating from the same vestibular imbalance that has been hypothesized to account for DBN in these and other cerebellar disorders (Baloh and Spooner 1981; Baloh and Yee 1989; Bohmer and Straumann 1998; Gresty et al. 1986). It is also possible that the static elevation reflects an imbalance of otolithic pathways engendered by dysfunction of the midline cerebellum (Mossman and Halmagyi 1997). The up/down asymmetry of vertical OKR gains raises still another possibility. The dominance of circuits participating in upward-directed OKR may drive the eyes upward until they come into equilibrium with the recentering forces dictated by the elasticity of the ocular motor plant. However, even though such an imbalance could contribute to the elevation in *tottering*, it is unlikely to be the sole explanation because, although *rocker* shares the hyperdeviation with *tottering*, it does not share the up/down asymmetry of OKR gains.

*Fast phase dynamics*

Slopes of the peak velocity versus amplitude relationships for fast phases of vestibular nystagmus were normal in the youngest *tottering* mutants, becoming moderately subnormal only with advancing age. These results contrast with those in *rocker*, in which fast phases were subnormal in all age groups. We investigated fast phase dynamics because, as a result of the appreciable viscous damping of the ocular motor plant, these rapid eye movements require far greater peak levels of muscular force than the slower compensatory eye movements. Thus if fast phase peak velocities are normal, it is less likely that a subnormality of the OKR or VOR is attributable to weakness arising from deficits of neuromuscular transmission (Leigh and Zee 1999; Stahl et al. 1998). Indeed, defects of neuromuscular transmission have been demonstrated in limb and diaphragmatic muscle of *tottering* mutants (Plomp et al. 2000, 2003), but if extraocular muscles share this defect, the preservation of saccade dynamics suggests it is without functional significance. The contrast between the slowed fast phases of *rocker* and the normal fast phases of young *tottering*—a mutant whose behavioral abnormalities are in all other respects more severe—is significant. First, if the attenuation of compensatory eye movements in *rocker* and *tottering* arises from the same cause, and if *tottering*'s more severe attenuation cannot be attributed to neuromuscular dysfunction, then *rocker*'s less severe gain deficits should not be attributed to neuromuscular dysfunction, either. Second, the evidence that *tottering*'s extraocular neuromuscular junctions are functionally normal argues for the integrity of *rocker*'s neuromuscular transmission as well, and thus the fast phase slowing in *rocker* may be attributable to abnormal firing rate patterns (e.g., weakness of the motoneuronal saccadic burst). This speculation is based on the observation that, in the murine Cacna1a mutants in which P/Q channel electrophysiology has been evaluated in vitro (*tottering*, *rolling-Nagoya*, *leaner*, and the $\alpha_{1A}$ null mutant), the severity of the electrophysiological abnormality correlates with the degree of ataxia (Mori et al. 2000). In vitro data are not available for *rocker*. However, if the pattern holds true, then its milder ataxia indicates that its P/Q calcium channels are more normal than those of *tottering*, and if neuromuscular transmission follows the same rank order as ataxia, then transmission deficits in *rocker* should be very mild and as functionally insignificant as they were in *tottering*. Ultimately, the source of *rocker*'s fast phase abnormality can be resolved by single-unit recordings from extraocular motoneurons because these data can determine whether the scaling from firing rate to eye velocity (a transformation dictated in part by neuromuscular transmission) is normal, and the same recordings can assess the normality of firing rate bursts associated with fast phases.

*Vestibular compensatory eye movements*

*Tottering* exhibited abnormalities of VOR gain and phase. The phase abnormalities are discussed with the neural integrator findings, below. Reductions in VOR gain were striking, particularly at the highest stimulus frequencies. *Rocker*'s gain attenuation at the highest stimulus frequencies was quantitatively similar to that found in *tottering*, but its gain was normal at the lowest frequencies. The attenuation is compatible with dysfunction of the cerebellar flocculus, which is believed to enhance VOR and/or OKR gain in afoveate mammals (Barmack and Pettorossi 1985; Ito 1982; Nagao 1983; van Neerven et al. 1989). The enhancement occurs, despite the fact that Purkinje cells are inhibitory, because the simple spike modulation of flocculus Purkinje cells is out of phase with the vestibular nucleus neurons that are its targets (De Zeeuw et al. 1995; Graf et al. 1988; Nagao 1989; Stahl and Simpson 1995). Although this statement is based on work in the rabbit, recent recordings in the mouse suggest that the phase of its floccular Purkinje cells is similar (Goossens et al. 2004; Hoebeek et al. 2005). The finding that the gain deficits in *rocker* and *tottering* are respectively restricted to, or most severe at, higher stimulus frequencies could arise for two reasons: *1*) the normal vestibulocerebellum may enhance gain preferentially at higher stimulus frequencies, and this normal function is impaired in the mutants; or *2*) the derangement of vestibulocerebellar signals in the mutants may occur predominantly at higher stimulus

frequencies. Some support for the first possibility comes from studies of the modulation phase of floccular Purkinje cells (De Zeeuw et al. 1995) and their vestibular targets (Stahl and Simpson 1995), which suggested that the afoveate flocculus normally provides a signal in which velocity components (i.e., high-frequency signals) are emphasized. Studies involving floccular lesions in afoveate mammals could potentially distinguish between the two possibilities. (If the first explanation is correct, the lesions would be expected to generate a VOR gain deficit that is more prominent at higher stimulus frequencies.) Unfortunately, the lesion studies published to date have assessed VOR gain over restricted ranges of stimulus frequency, or at frequencies lower than those used in the current study (Nagao 1983; van Neerven et al. 1989), or explored the effects of unilateral lesions only (Barmack and Pettorossi 1985; Ito et al. 1982), or used eye movement recording techniques (Koekkoek et al. 1997) that subsequently were demonstrated to be problematic (Stahl et al. 2000). Future recordings of floccular Purkinje cell modulation during VOR in control mice and Cacna1a mutants could provide more insight into the problem by determining whether the floccular modulation in mutants is subnormal and whether such subnormality exhibits a frequency dependency similar to that of the behavioral deficit.

We also investigated the geometry of the vestibular-induced compensatory eye movements using the "thrust" test. We predicted that there would be misalignments between the axes of the head rotation and evoked eye movement, based on the demonstration of misalignments of VOR in humans with cerebellar disorders (Walker and Zee 1999; Zee et al. 2002). The result was complex: *tottering* mutants were actually better aligned as a group than were controls and, although *rocker* was less aligned in terms of the angular deviation from the ideal horizontal response, the difference appeared to arise from the reduction in the horizontal component of the response, rather than an increase in the magnitude of the inappropriate vertical component. Even if we consider only *rocker*'s angular deviation with respect to controls, the result is different from the finding in humans, in which thrusts to *either* side engendered an inappropriate *upward* component of eye movement, indicating a nonlinearity in the pathophysiological mechanism. In contrast, we found a linear effect, in which ipsilateral thrusts generated a downward, and contralateral thrusts an upward, deviation. Walker also found a linear component to the distortion of the response axis, in which rightward and leftward eye movements were associated respectively with inappropriate clockwise and counterclockwise components. Our results were based on 2D recordings; because the mouse optical axis lies approximately midway between the nasooccipital and bitemporal axes, the vertical movements in *rocker* could represent a cross-coupling to either of these axes. However, if we assume, as in humans, the coupling is to the nasooccipital axis (the torsion axis in humans), then rightward movements (adducting movements in the left eye) were associated with counterclockwise motion about the nasooccipital axis, in short, the reverse of the finding in humans. In sum, the results of the thrust experiments were subtle and their correspondence to findings in humans uncertain. Further exploration of these phenomena will likely require the development of three-dimensional videooculography techniques suitable for use in mice.

### *Optokinetic compensatory eye movements*

*Tottering* exhibited horizontal optokinetic defects that may reflect a combination of congenital and acquired processes. Evidence of a congenital gain deficit included the significant differences between the speed-tuning curves of *tottering* and control at the youngest age studied, as well as the failure of the gain versus age regression curves to fully converge at their *y*-intercepts. Evidence for an acquired component included the downward trends of the gain versus age plots, as well as the widening with age of the gap between mutant and control VVOR gains at low stimulus frequencies, where eye movements are dominated by the OKR. Although the combination of congenital and progressive deficits suggests the existence of separable congenital and acquired pathological mechanisms, we cannot exclude the possibility that a single, progressive mechanism is established long before the earliest age we studied, and so simulates the presence of a congenital deficit. Vertical OKR gains also showed a consistent tendency to decline with age. In contrast, the data did not support an argument for or against the existence of an additional congenital deficit because for some speeds/directions the vertical gain versus age regression curves converged at birth, whereas in other cases the *y*-intercepts differed significantly. The deficiencies in horizontal OKR accord with previous studies of ataxic mouse mutants (van Alphen et al. 2002) and flocculus lesion studies in afoveates (Barmack and Pettorossi 1985; Ito et al. 1982; Koekkoek et al. 1997; Nagao 1983; van Neerven et al. 1989), indicating that the neural signals supporting the afoveate OKR traverse the cerebellar flocculus or, conversely, that the ocular motor deficits in Cacna1a mutants reflect, at least in part, floccular dysfunction.

A striking observation from these experiments was the degree to which *tottering* exhibits directional asymmetries of OKR gain, both for horizontal and vertical (roll axis) stimulation. Gains were lower for nasally than for temporally directed OKR, and for downward than for upward OKR (all with respect to the recorded eye). In comparison to *tottering*, normal mice and *rocker* mutants exhibited symmetrical horizontal and vertical OKR gains. Likewise the rabbit, another afoveate mammal and one whose ocular motor performance has been studied extensively, exhibits symmetrical horizontal and vertical optokinetic gains during binocular stimulation (Collewijn 1969; Collewijn and Noorduin 1972; Tan et al. 1993). In the course of investigating the asymmetry, we tested the effects of presenting different optokinetic stimuli to the two eyes. These experiments—the first of their kind in the mouse—demonstrated that the eye is ordinarily driven most strongly by its own optokinetic stimulation and that the influence of the contralateral eye is strongest during its exposure to temporal-nasal stimulation. Of note, the symmetry in control animals during monocular stimulation contrasts with the situation in the rabbit, in which nasal-temporal responses to rotation speeds $>1°/s$ are weak (Collewijn 1969), and thus in the rabbit the nasal-temporal response during binocular stimulation is driven almost exclusively by the concurrent temporal-nasal stimulation of the contralateral eye. Mice also exhibited the influence of the contralateral eye during its temporal-nasal stimulation, although it appeared to play a smaller role in the symmetry of the response to binocular stimulation. We were able to exclude the possibility that *tottering*'s asymmetry reflects a failure to

sustain nasally directed eye velocities, the failure arising from the long *duration* of the constant velocity optokinetic stimulus. This analysis, however, does not exclude the possibility of a failure to sustain eye velocities arising from the large *amplitudes* of eye movement evoked by the OKR stimulus. For instance, if *tottering*'s OKR gain falls as a function of nasal eccentricity within the orbit, the effect might be revealed by the unidirectional OKR stimulus but not the oscillatory, lower-amplitude VOR and VVOR stimuli. This possibility could be assessed by testing the VOR under the analogous condition of constant acceleration.

Although the etiology of the horizontal and vertical optokinetic asymmetries remains conjectural, the data provide several constraints on the potential mechanism. First, because the animal-to-animal variations in nasally and downward-directed OKR gains were correlated, the asymmetries in the two axes may arise from a common pathophysiological mechanism. Second, the mechanism is likely an acquired, or at least progressive, process because the deficiencies in nasally and downward-directed OKR gains became more prominent with aging. Third, because VOR and VVOR gains in the horizontal plane exhibited an asymmetry opposite to that of the OKR, the abnormality underlying OKR asymmetries must reflect the operation of a pathway or mechanism not associated with, or invoked by, the oscillatory VOR and VVOR stimuli. Fourth, because *rocker* shared the attenuation of the VOR but not the optokinetic asymmetries, the mechanisms of these vestibular and optokinetic abnormalities are likely to be distinct. Fifth, the asymmetry cannot arise from a general reduction of the inhibitory tone emanating from the flocculus. Because stimulation of floccular microzones in afoveates produces variously abduction or depression of the ipsilateral eye (van der Steen et al. 1994), a reduction in the average firing rate would engender an upward bias (which could contribute to the reduction of downward gain) but also a nasally directed bias (which would contribute to a relative reduction of nasal-temporal, not temporal-nasal gain).

Recordings of Purkinje cells in *tottering* during constant velocity OKR could provide further insight into the site of dysfunction. For instance, reduced transmission of visuomotor signals to the flocculus would reduce modulation amplitudes during nasally directed OKR compared with controls. In contrast, a defect lying downstream to the Purkinje cell spike initiation zone would not affect modulation amplitude, but it would *increase* the ratio of modulation and eye movement amplitudes. Finally, it should be noted that humans with cerebellar disorders have been shown to have specific impairments of downward smooth pursuit gain, and the abnormality has also been attributed to abnormalities of the flocculus (Glasauer et al. 2005). However, a direct relationship between the mechanisms underlying the vertical OKR deficit in mice and the smooth pursuit deficit in humans is problematic because mice (like other afoveate mammals) lack the ability to perform smooth pursuit.

### *Neural integrator dysfunction*

*Tottering* exhibited an increase in VOR phase lead at low stimulus frequencies, an abnormality that was also found in the previous study of *rocker* (Stahl 2004a). We previously speculated that these excessive phase leads reflected abnormal "leakiness" (i.e., a reduced time constant) of the neural integrator. The integrator acts to generate a neural signal proportional to desired eye position, and in the process adds lag to the phase relationship between head velocity and extraocular motoneuron firing (Skavenski and Robinson 1973). As such, a shorter integrator time constant would reduce that normal lag and thereby increase the lead of eye velocity with respect to head velocity during rotation in darkness. Direct assessment of the integrator time constant in control animals demonstrated a wide degree of variability. Some of this variability may reflect limitations of the analysis (see following text). However, it may also be that this aspect of the mouse ocular motor repertoire is not maintained under tight control, if the short average values [which are as little as one tenth the values obtained in the primate (Cannon and Robinson 1987)] indicate that eccentric gaze holding is of relatively little importance to the mouse. In any case, the average time constants of control animals were clearly greater than those of both *tottering* and *rocker*. The difference is sufficient to explain approximately one half of the abnormal phase lead of the mutants. Animal-to-animal variations of time constant and phase lead did not correlate. The lack of correlation could indicate that the increased phase lead does not, after all, arise from integrator dysfunction. However, the lack of correlation could also arise because of the degree of independent variability inherent in both of these measures. The phase measure is variable because the amplitude of the VOR is very low at 0.1 Hz, and thus strongly influenced by any random aspects of the behavior, even when several cycles of response are averaged. Time constant measurements are subject to both biological and analytical sources of variation. The single exponential decay to a central position and a rigidly constant time "constant" are only rough approximations of the range of actual behavior. In practice, there is considerable trial-to-trial variability of the time constant. In addition, some drifts appear linear, some are associated with midcourse accelerations/decelerations, some appear to be multiexponential, and in some cases the drifts halt far from the central eye position. Although we used a set of criteria to focus our curve fitting on responses with a grossly exponential profile, a wide latitude was permitted. When the actual decay fits the form of a single exponential imperfectly, the curve fitting becomes less stable, prone to being influenced by features of each curve that are effectively random with respect to the average exponential behavior. Because these causes of phase and time constant variability are unrelated, they would be expected to mask any correlation between the two variables.

Lesion experiments in primates have suggested that the cerebellar flocculus augments the neural integrator time constant. In nonprimates the picture is less clear because lesion studies have generated data that argue both for (Chelazzi et al. 1990) and against (Ito et al. 1982; Koekkoek et al. 1997; Nagao 1983) a floccular contribution to the neural integrator. Moreover, recordings in the rabbit flocculus and its brain stem synaptic targets indicate that the flocculus conveys a less, rather than more, integrated version of the premotor command (De Zeeuw et al. 1995; Stahl and Simpson 1995). The current results support a role for the afoveate flocculus in supporting integrator function [provided that the behavioral abnormality stems from mutated channels in the cerebellum, where P/Q calcium channels are heavily distributed, as opposed to the

brain stem, where they are only lightly expressed (Craig et al. 1998; Hillman et al. 1991; Stea et al. 1994)]. Because cerebellar defects in *tottering* and *rocker* would relate to *abnormal* floccular signals, as opposed to the *absence* of floccular signals engendered in anatomical and pharmacological lesion experiments, these mutants provide the opportunity, by recordings of normal and mutant floccular Purkinje cells, to investigate what aspect of floccular output is responsible for augmenting integrator function.

Of note, the current study is the first in which the integrator time constant was assessed in an afoveate using noninvasive oculography, and the values were slightly longer than the 2.1-s value reported in a previous study of mice recorded using search coil oculography (van Alphen et al. 2001). Because implanting search coils has also been shown to increase phase lead of the VVOR (Stahl et al. 2000), some of the difference in integrator time constants likely stems from mechanical effects of a foreign body implanted in the orbit.

### *VOR adaptation*

The ability of the VOR circuits to adjust their gain is essential to the production of compensatory eye movements of proper amplitude and direction. The cerebellar flocculus is well known to participate in this adjustment process (duLac et al. 1995; Ito 1982; Miles and Lisberger 1981; Schultheis and Robinson 1981), and thus deficits in cross-axis plasticity are consistent with floccular dysfunction. Previously we demonstrated that cross-axis adaptation was severely impaired in *rocker* mutants (Stahl 2004a). The current experiments demonstrated that in *tottering*, a more severely affected Cacna1a mutant, cross-axis adaptation was entirely absent. Although these results accord with the ideas that the flocculus underlies vestibular plasticity and Cacna1a mutations impair its function, some caution is warranted because the mutants generated poor (or, in the case of *tottering*, no) vertical eye movements in response to the adapting stimulus. The poor response raises the possibility that an optokinetic defect is responsible for the failure to adapt, although there are also arguments against this explanation. First, we found no correlation within strains between the variations in initial vertical response and the degree of adaptation. Second, the roll optokinetic speed-tuning curves do not support a simple failure of vertical optokinetic pathways. *Tottering* did exhibit reductions of vertical OKR, but we restricted the cross-axis analysis to the youngest age group, in which the impairment of OKR was slight over the stimulus speeds used in the cross-axis paradigm. *Rocker*'s vertical OKR gain was comparable to that of controls in the youngest age group, and entirely normal in the oldest animals (no statement can be made regarding the normality of the middle age group because comparative data from control animals were not obtained). Thus the degree of impairment of adaptation seems disproportionate to the deficiencies of OKR in either mutant. This argument, of course, rests on the tacit assumption of a connection between the responses to the sinusoidal optokinetic stimuli used to generate cross-axis adaptation and the constant velocity stimuli used to generate the speed-tuning curves. The assumption is plausible because plots of sinusoidal gain versus stimulus frequency in the rabbit collapse into single curves when gain is plotted versus peak velocity, arguing that velocity, not stimulus frequency, largely dictates the optokinetic response (Collewijn 1981). Nevertheless, a comparable exploration of the relationship between sinusoidal and constant velocity vertical OKR has yet to be performed in the mouse.

Another difference between *tottering* and control animals that might bear on the cross-axis results is that, according to the thrust experiments, control animals, but not *tottering*, possess a tendency to generate downward motion during adducting eye movements. The cross-axis adaptation seen in control animals might represent a strengthening of this baseline cross-coupling, and *tottering*'s inability to adapt might then reflect the lack of the baseline cross-coupling. However, *rocker* did exhibit the cross-coupling in the thrust experiments, and parsimony would argue against invoking a mechanism to explain a deficit in *tottering* that could not also be applied to *rocker*. Ultimately, it may be possible to investigate the adaptation—and its deficiency in Cacna1a mutants—using single-neuron recordings because the cross-coupling develops sufficiently rapidly that it should be possible to monitor changes in activity of a single neuron as the cross-coupling progresses.

### *Multiplicity of mechanisms accounting for ocular motor deficits in mutants*

As noted in the INTRODUCTION, Cacna1a mutations have the potential to engender a wide variety of effects, beginning with a multiplicity of alterations of channel biophysics and leading, at a more macroscopic level, to various alterations of synaptic transmission, dendritic excitability, and network-level effects. In addition to these direct effects, the mutations may also engender lifelong secondary adaptive phenomena, such as the substitution of N-type for P/Q-type calcium channels in the synaptic apparatus (Zhou et al. 2003), as well as acquired effects, such as dendritic atrophy seen in aged *rocker* mutants (Zwingman et al. 2001) and cerebellar cortical degeneration that appears in *leaner* after P10 (Herrup and Wilczynski 1982). The distinct pathophysiological consequences might be expected to have differing behavioral effects and, indeed, the current behavioral data allow us to posit the existence of several distinctive pathophysiological mechanisms. These speculations draw support from three sources: from the correlations between different ocular motor measures, from a comparison of the effects of aging on the various abnormalities, and from comparisons between mutant strains.

Correlations between abnormal parameters within a strain provide the least powerful evidence of distinct pathophysiological mechanisms. Two behavioral abnormalities can arise from the same mechanism, but if the *variations* in the two behavioral indices are not driven by variations in the severity of the common mechanism but rather, by random influences, measurement uncertainty, or analytical sources of variability peculiar to each of the behavioral indices, then the two indices will fail to correlate. This confound has been suggested above as a possible explanation for the failure to detect a correlation between the integrator time constant and the VOR phase lead at low stimulus frequencies. Correlation analysis is most useful when two parameters *do* correlate, in which case it is at least possible that the two abnormalities (or, at least, the sources of their variability) ultimately *do* stem from a common mechanism. Thus we can provisionally posit two mechanisms acting in *tottering* on the basis of the correlation analysis, including: *1*) a mechanism accounting for reductions in temporal-nasal

and downward optokinetic gains, as well as static hyperdeviation of the eyes; and *2*) a mechanism accounting for generalized (symmetrical) attenuation of horizontal and vertical OKR and of horizontal VOR.

Observations of the effects of age on ocular motor indices allow us to distinguish between abnormalities that are potentially congenital versus definitely acquired and thus to posit the existence of distinguishable congenital versus acquired pathophysiological mechanisms. As in the case of the correlations between parameters discussed above, some caution is warranted when attempting to distinguish between congenital and acquired abnormalities on the basis of regressing ocular motor measures versus age. For instance, one cannot conclude definitively that a given defect is congenital because it is always possible that the defect was simply acquired before the youngest age studied. Because mouse eye movements cannot be recorded at birth, this problem is essentially intractable. Thus all the "congenital" defects we describe are, in fact, only "provisionally congenital," although we have omitted repeating the qualifying adverb for the sake of brevity. What can be said with confidence is that abnormalities that were documented in 2- to 8-mo-old animals are unlikely to be related to known acquired alterations that have been demonstrated only in elderly animals (such as dendritic weeping in *rocker*). It should also be recognized that the claim that an abnormality is "acquired" does not necessarily exclude a direct role of the mutation-induced alterations in channel biophysics. For instance, if the levels of channel expression in mutants change with age (a possibility yet to be explored in either the human or animal literature), the biophysical consequences of the mutation may appear in a delayed fashion. However, in this case it should be recognized that, ultimately, the appearance of the abnormality reflects the conjunction of the congenital biophysical abnormality and an *acquired* change in expression, and thus our statement in the INTRODUCTION that an acquired abnormality should not arise *exclusively* from a congenital abnormality.

With these caveats in mind, we can state that the defects in *tottering* that are most likely to be congenital include the attenuation of VOR, increases in VOR phase lead at low stimulus frequencies, decreases in the time constant of the neural integrator, a slightly abnormal alignment of VOR response axes during rapid rotation, and deficient cross-axis plasticity. Whether there is a congenital component to the horizontal OKR gain deficit is less clear. The significant difference between the y-intercepts of *tottering* and controls in plots of temporal-nasal gains versus age suggests there is a congenital component, but the plots' consistent negative slopes suggest an acquired deficit as well. Thus horizontal OKR gains could reflect a mixture of congenital and acquired deficits, or an acquired deficit whose temporal course merely simulates an additional congenital defect. There was less evidence to support a congenital component to the overall vertical OKR gain deficit. As with the horizontal OKR gain deficit, the natural history of the static hyperdeviation in *tottering* is uncertain. On one hand, the presence of the hyperdeviation at the earliest age we studied and the nonsignificance of the correlation between elevation and age argue for a purely congenital abnormality. On the other hand, elevation does trend upward with age, and the nonsignificance of this trend could simply reflect the high degree of animal-to-animal variability.

Contrasts between the defects of *rocker* and *tottering* provide the third set of clues to the existence of distinctive pathophysiological mechanisms. A mechanism must be postulated to account for the congenital slowing of fast phases in *rocker*, and is apparently peculiar to this strain. Likewise, the mechanism underlying asymmetries of OKR gain must be peculiar to *tottering*. Qualitative similarities between the two strains suggest the existence of shared physiological abnormalities, including those responsible for deficiencies of VOR (particularly at high stimulus frequencies), symmetrical reductions of OKR, static hyperdeviation, neural integrator dysfunction, and reduced plasticity. In one case the correlation data and cross-strain comparisons generate conflicting implications for the number of mechanisms at work: The correlation analysis indicates that, in *tottering*, static hyperdeviation is linked to the asymmetry of vertical OKR, but in *rocker* the static hyperdeviation was observed despite the lack of the vertical OKR asymmetry.

In sum, taking the correlation, aging, and cross-strain data together, there is tentative support for at least four pathological processes affecting ocular motility in Cacna1a mutants: *1*) at least one congenital process resulting in deficient VOR gain, some of the deficiency in OKR gain, leakiness of the neural integrator, and reduced cross-axis plasticity; *2*) a process, probably acquired, producing static hyperdeviation; *3*) a process, peculiar to *tottering* and either acquired or progressive, that produces asymmetries of OKR gain and possibly contributes to *tottering*'s more severe static hyperdeviation. This process may localize to a point within the circuitry before vestibular and visuomotor signals become fully commingled because the VOR does not share with the OKR the reduction in temporal-nasal gains; and *4*) a congenital process producing slowed fast phases of nystagmus in *rocker*.

### *Relationships to data emerging from single-neuron recordings*

Recently, recordings have been performed in floccular Purkinje cells of *tottering* mutants and C57BL/6 controls at rest and during OKR (Hoebeek et al. 2005). This study demonstrated that *tottering* Purkinje cells exhibit unusual degrees of firing rate irregularity, both at rest and during modulation. The modulation amplitude, however, was normal, arguing against OKR gain deficits arising from a failure of visuomotor signals to be communicated to Purkinje cells arising from mutated P/Q calcium channels interfering with synaptic transmission. The same study demonstrated, by electrical stimulation of the flocculus, that Purkinje cell terminals in *tottering* are capable of transmitting signals to their brain stem targets, and that both flocculus lesions and intrafloccular injection of P/Q channel antagonists impair OKR in control animals but not *tottering* mutants, providing further evidence that the flocculus in normal animals supports the OKR, and that this function is apparently absent in *tottering* mutants. Hoebeek and colleagues concluded from these data that the greater irregularity of *tottering* Purkinje cells in some way functionally nullifies the floccular outputs.

The juxtaposition of the results of Hoebeek and colleagues with the current behavioral data raises a number of intriguing questions. First, do the floccular Purkinje cells in *rocker* share the increased irregularity seen in *tottering* and is the irregular-

ity in *rocker* of a lesser degree, in parallel with the more moderate nature of the ocular motor and gait abnormalities in this strain? As argued in the INTRODUCTION, a given neuronal abnormality is more likely to account for a behavioral abnormality if the severities of the neuronal and behavioral abnormalities vary proportionately across allelic mutants. Second, how does an increase in irregularity account for the strong frequency dependency of the VOR deficits in both *rocker* and *tottering*? One possibility to consider is that the increased irregularity degrades the ability of the flocculus to encode information on short timescales and thus preferentially impairs the VOR at high stimulus frequencies. However, this explanation would not easily account for the correlated reductions in OKR gain, which were demonstrated using constant velocity (i.e., DC) stimuli, nor would it easily explain the deficits in another ocular motor function associated with low rates of eye position variation, neural integrator function. Further insight into the connections between firing rate irregularity and floccular function will likely be gained by experiments aimed at comparing floccular modulation during optokinetic and vestibular stimulation in *tottering*, or assessing the parallels between the frequency dependency of firing rate irregularity and VOR gain in *rocker*.

As noted in the INTRODUCTION, P/Q calcium channels are expressed at a variety of locations and thus could exert their deleterious effects by a variety of mechanisms. Indeed, we have already inferred the existence of several distinctive mechanisms on the basis of the behavioral observations. The finding of greater irregularity in *tottering* floccular Purkinje cells, however, increases the likelihood that deranged dendritic integration is an important factor in the ocular motor dysfunction of Cacna1a mutants. Given the strong degree of convergence of parallel fibers on Purkinje cells [each Purkinje cell receives synapses from approximately 175,000 granule cells (Napper and Harvey 1988)], it is difficult to see how a high degree of irregularity in individual parallel fibers could be transferred to the Purkinje cell; so long as firing is not synchronized across the parallel fibers, irregularities would be expected to average out as impulses summate on the Purkinje cell. Nor is it clear how a reduced efficiency of the parallel fiber's synapse on the Purkinje cell (Matsushita et al. 2002) would engender greater irregularity once that transmission deficit was averaged across a large number of converging parallel fibers. More plausible is the idea that the irregularity stems from altered excitability of the Purkinje cell dendrite, which in turn may arise because reduced calcium influx leads to reduced activity of the calcium-dependent potassium channel, the major restabilizing influence on the dendritic membrane potential (De Schutter and Bower 1994; Jacquin and Gruol 1999; Llinas and Sugimori 1980).

The argument from the single-neuron data can be joined to a more circumstantial argument for behavioral derangements arising from altered dendritic signaling. All Cacna1a mutants exhibit motor abnormalities that have been interpreted as cerebellar ataxia, whereas other phenotypic stigmata are more variable (Zwingman et al. 2001). The degree to which *rocker* and *tottering* exhibit normal behaviors such as grooming, feeding, and breeding (Green and Sidman 1962; Zwingman et al. 2001) suggests that the impact, in functional terms, of the mutant P/Q calcium channels found on synapses throughout the brain is mild, either because compensatory mechanisms (such as upregulation of N-type calcium channels) rescue this function or because the safety factor of synaptic transmission is sufficient to prevent a small reduction of calcium currents from having a functional impact. In contrast, the commonality of cerebellar ataxia suggests that some function other than synaptic transmission and unique to the cerebellum is particularly sensitive to Cacna1a mutations. The Purkinje cell dendrite, with its regenerative P/Q calcium currents, is thus a prime candidate for this sensitive site. Furthermore, the degree to which its architectural and biophysical peculiarities have been conserved through evolution (Midtgaard 1994; Smith et al. 1993) only renders it more likely that modifications of these conserved elements would have deleterious effects on its computational functions. In sum, a variety of evidence supports the idea that Cacna1a mutants may provide examples of deranged dendritic signal processing and their investigation may lead to a better understanding of the vestibulocerebellar contribution to ocular motor control.

## ACKNOWLEDGMENTS

The authors gratefully acknowledge T. Zwingman for providing mice to found the *tottering* colony, as well as advice regarding their husbandry and genetics. The guidance and encouragement of K. Herrup were instrumental in the early stages of formulating this project.

## GRANTS

This work was supported by National Eye Institute Grants EY-13370 and EY-11373 and the U.S. Department of Veterans Affairs. C. I. De Zeeuw and F. E. Hoebeek were supported by Neuro-Besluit subsidies investeringen kennisinfrastructuur, The Netherlands Organisation for Health Research and Development, The Netherlands Organisation for Scientific Research–Earth and Life Sciences, The Netherlands Organisation for Scientific Research–Personal Impulse for Research Groups with New Ideas for Excellent Research, and European Economic Community.

## REFERENCES

**Ashcroft F.** *Ion Channels and Disease.* San Diego, CA: Academic Press, 2000.

**Baloh RW and Spooner JW.** Downbeat nystagmus: a type of central vestibular nystagmus. *Neurology* 31: 304–310, 1981.

**Baloh RW and Yee RD.** Spontaneous vertical nystagmus. *Rev Neurol* (*Paris*) 145: 527–532, 1989.

**Barmack NH and Pettorossi VE.** Effects of unilateral lesions of the flocculus on optokinetic and vestibuloocular reflexes of the rabbit. *Ann NY Acad Sci* 53: 481–496, 1985.

**Bohmer A and Straumann D.** Pathomechanism of mammalian downbeat nystagmus due to cerebellar lesion: a simple hypothesis. *Neurosci Lett* 250: 127–130, 1998.

**Caddick SJ, Wang C, Fletcher CF, Jenkins NA, Copeland NG, and Hosford DA.** Excitatory but not inhibitory synaptic transmission is reduced in lethargic (Cacnb4-lh) and tottering (Cacna1a-tg) mouse thalami. *J Neurophysiol* 81: 2066–2074, 1999.

**Caddy KW and Biscoe TJ.** The number of Purkinje cells and olive neurones in the normal and Lurcher. *Brain Res* 111: 396–398, 1976.

**Cannon SC and Robinson DA.** Loss of the neural integrator of the oculomotor system from brain stem lesions in monkey. *J Neurophysiol* 57: 1383–1409, 1987.

**Chelazzi L, Ghirardi M, Rossi F, Strata P, and Tempia F.** Spontaneous saccades and gaze-holding ability in the pigmented rat. II. Effects of localized cerebellar lesions. *Eur J Neurosci* 2: 1085–1094, 1990.

**Cicale M, Ambesi-Impiombato A, Cimini V, Fiore G, Muscettola G, Abbott LC, and de Bartolomeis A.** Decreased gene expression of calretinin and ryanodine receptor type 1 in tottering mice. *Brain Res Bull* 59: 53–58, 2002.

**Collewijn H.** Optokinetic eye movements in the rabbit: input–output relations. *Vision Res* 9: 117–132, 1969.

**Collewijn H.** *The Oculomotor System of the Rabbit and Its Plasticity.* New York: Springer-Verlag, 1981.

**Collewijn H and Noorduin H.** Vertical and torsional optokinetic eye movements in the rabbit. *Pfluegers Arch* 332: 87–95, 1972.

**Craig PJ, McAinsh AD, McCormack AL, Smith W, Beattie RE, Priestley JV, Yip JLY, Averill S, Longbottom ER, and Volsen SG.** Distribution of the voltage-dependent calcium channel alpha1A subunit throughout the mature rat brain and its relationship to neurotransmitter pathways. *J Comp Neurol* 397: 251–267, 1998.

**De Schutter E and Bower JM.** An active membrane model of the cerebellar Purkinje cell. II. Simulation of synaptic responses. *J Neurophysiol* 71: 401–419, 1994.

**De Zeeuw CI, Wylie DR, Stahl JS, and Simpson JI.** Phase relations of Purkinje cells in the rabbit flocculus during compensatory eye movements. *J Neurophysiol* 74: 2051–2064, 1995.

**Dove LS, Nahm S-S, Murchison D, Abbott LC, and Griffith WH.** Altered calcium homeostasis in cerebellar Purkinje cells of leaner mutant mice. *J Neurophysiol* 84: 513–524, 2000.

**duLac S, Raymond JL, Sejnowski TJ, and Lisberger SG.** Learning and memory in the vestibulo-ocular reflex. *Annu Rev Neurosci* 18: 409–441, 1995.

**Glasauer S, Hoshi M, and Buttner U.** Smooth pursuit in patients with downbeat nystagmus. *Ann NY Acad Sci* 1039: 532–535, 2005.

**Goossens HHLM, Hoebeek FE, van Alphen AM, van der Steen J, Stahl JS, De Zeeuw CI, and Frens MA.** Simple spike and complex spike activity of floccular Purkinje cells during the optokinetic reflex in mice lacking cerebellar LTD. *Eur J Neurosci* 19: 687–697, 2004.

**Graf W, Simpson JI, and Leonard CS.** Spatial organization of visual messages of the rabbit's cerebellar flocculus. II. Complex and simple spike responses of Purkinje cells. *J Neurophysiol* 60: 2091–2121, 1988.

**Green M and Sidman R.** Tottering—a neuromuscular mutation in the mouse and its linkage with oligosyndactylism. *J Hered* 58: 233–237, 1962.

**Gresty MA, Barratt H, Rudge P, and Page N.** Analysis of downbeat nystagmus: otolithic vs. semicircular canal influences. *Arch Neurol* 43: 52–55, 1986.

**Herrup K and Wilczynski SL.** Cerebellar cell degeneration in the leaner mutant mouse. *Neuroscience* 7: 2185–2196, 1982.

**Hillman D, Chen S, Aung TT, Cherksey B, Sugimori M, and Llinas RR.** Localization of P-type calcium channels in the central nervous system. *Proc Natl Acad Sci USA* 88: 7076–7080, 1991.

**Hoebeek FE, Stahl JS, van Alphen AM, Schonewille M, Luo C, Rutteman M, van den Maagdenberg AM, Molenaar PC, Goosens HH, Frens MA, and De Zeeuw CI.** Increased noise level of Purkinje cell activities can cancel impact of their modulation during sensorimotor control. *Neuron* 45: 953–965, 2005.

**Isaacs KR and Abbott LC.** Development of the paramedian lobule of the cerebellum in wild-type and tottering mice. *Dev Neurosci* 14: 386–393, 1992.

**Ito M.** Cerebellar control of the vestibulo-ocular reflex—around the flocculus hypothesis. *Annu Rev Neurosci* 5: 275–296, 1982.

**Ito M, Jastreboff PJ, and Miyashita Y.** Specific effects of unilateral lesions in the flocculus upon eye movements in albino rabbits. *Exp Brain Res* 45: 233–242, 1982.

**Jacquin TD and Gruol DL.** $Ca^{2+}$ regulation of a large conductance $K^+$ channel in cultured rat cerebellar Purkinje cells. *Eur J Neurosci* 11: 735–739, 1999.

**Jaeger D, De Schutter E, and Bower JM.** The role of synaptic and voltage-gated currents in the control of Purkinje cell spiking: a modeling study. *J Neurosci* 17: 91–106, 1997.

**Kaufman GD.** Video-oculography in the gerbil. *Brain Res* 958: 472–487, 2002.

**Koekkoek SKE, Alphen AM, van der Burg J, Grosveld F, Galjart N, and De Zeeuw CI.** Gain adaptation and phase dynamics of compensatory eye movements in mice. *Genes Funct* 1: 175–190, 1997.

**Leigh RJ and Zee DS.** *The Neurology of Eye Movements.* New York: Oxford Univ. Press, 1999.

**Leonard CS, Simpson JI, and Graf W.** Spatial organization of visual messages of the rabbit's cerebellar flocculus. I. Typology of inferior olive neurons of the dorsal cap of Kooy. *J Neurophysiol* 60: 2073–2090, 1988.

**Llinas R and Moreno H.** Local $Ca^{2+}$ signaling in neurons. *Cell Calcium* 24: 359–366, 1998.

**Llinas R and Sugimori M.** Electrophysiological properties of *in vitro* Purkinje cell dendrites in mammalian cerebellar slices. *J Physiol* 305: 197–213, 1980.

**Llinas R, Sugimori M, Lin JW, and Cherksey B.** Blocking and isolation of a calcium channel from neurons in mammals and cephalopods utilizing a toxin fraction (FTX) from funnel-web spider poison. *Proc Natl Acad Sci USA* 86: 1689–1693, 1989.

**Matsushita K, Wakamori M, Rhyu IJ, Arii T, Oda S-i, Mori Y, and Imoto K.** Bidirectional alterations in cerebellar synaptic transmission of tottering and rolling $Ca^{2+}$ channel mutant mice. *J Neuroscience* 22: 4388–4398, 2002.

**Midtgaard J.** Processing of information from different sources: spatial synaptic integration in the dendrites of vertebrate CNS neurons. *Trends Neurosci* 17: 166–173, 1994.

**Miles FA and Lisberger SG.** Plasticity in the vestibulo-ocular reflex: a new hypothesis. *Annu Rev Neurosci* 4: 273–299, 1981.

**Mori Y, Wakamori M, Oda SI, Fletcher CF, Sekiguchi N, Mori E, Copeland NG, Jenkins NA, Matsushita K, Matsuyama Z, and Imoti K.** Reduced voltage sensitivity of activation of P/Q-Type $Ca^{2+}$ channels is associated with the ataxic mouse mutation rolling Nagoya (tg(rol)). *J Neurosci* 20: 5654–5662, 2000.

**Mossman S and Halmagyi GM.** Partial ocular tilt reaction due to unilateral cerebellar lesion. *Neurology* 49: 491–493, 1997.

**Murchison D, Dove LS, Abbott LC, and Griffith WH.** Homeostatic compensation maintains $Ca^{2+}$ signaling functions in Purkinje neurons in the leaner mutant mouse. *Cerebellum* 1: 119–127, 2002.

**Nagao S.** Effects of vestibulocerebellar lesions upon dynamic characteristics and adaptation of vestibulo-ocular and optokinetic responses in pigmented rabbits. *Exp Brain Res* 53: 36–46, 1983.

**Nagao S.** Behavior of floccular Purkinje cells correlated with adaptation of vestibulo-ocular reflex in pigmented rabbits. *Exp Brain Res* 77: 531–540, 1989.

**Napper RM and Harvey RJ.** Number of parallel fiber synapses on an individual Purkinje cell in the cerebellum of the rat. *J Comp Neurol* 274: 168–177, 1988.

**Plomp J, van den Maagdenberg A, Ferrari M, Frants RR, and Molenaar P.** Transmitter release deficits at the neuromuscular synapse of mice with mutations in the Cav2.1 (alpha1A) subunit of the P/Q-type $Ca^{2+}$ channel. *Ann NY Acad Sci* 998: 29–32, 2003.

**Plomp JJ, Vergouwe MN, Maagdenberg AMVd, Ferrari MD, Frants RR, and Molenaar PC.** Abnormal transmitter release at neuromuscular junctions of mice carrying the *tottering* $alpha_{1A}$ $Ca^{2+}$ channel mutation. *Brain* 123: 463–471, 2000.

**Rhyu I, Nahm S, Hwang S, Kim H, Suh Y, Oda S, Frank T, and Abbott L.** Altered neuronal nitric oxide synthase expression in the cerebellum of calcium channel mutant mice. *Brain Res* 977: 129–140, 2003.

**Rhyu IJ, Abbott LC, Walker DB, and Sotelo C.** An ultrastructural study of granule cell/Purkinje cell synapses in tottering (tg/tg), leaner (tg(la)/tg(la)) and compound heterozygous tottering/leaner (tg/tg(la)) mice. *Neuroscience* 90: 717–728, 1999.

**Schultheis L and Robinson D.** Directional plasticity of the vestibuloocular reflex in the cat. *Ann NY Acad Sci* 374: 504–512, 1981.

**Skavenski AA and Robinson DA.** Role of abducens neurons in vestibulooocular reflex. *J Neurophysiol* 36: 724–738, 1973.

**Smith TGJ, Brauer K, and Reichenbach A.** Quantitative phylogenetic constancy of cerebellar Purkinje cell morphological complexity. *J Comp Neurol* 331: 402–406, 1993.

**Stahl JS.** Calcium channelopathy mutants and their role in ocular motor research. *Ann NY Acad Sci* 956: 64–74, 2002.

**Stahl JS.** Eye movements of the murine P/Q calcium channel mutant rocker, and the impact of aging. *J Neurophysiol* 91: 2066–2078, 2004a.

**Stahl JS.** Using eye movements to assess brain function in mice. *Vision Res* 44: 3401–3410, 2004b.

**Stahl JS, Averbuch-Heller L, Remler BF, and Leigh RJ.** Clinical evidence of extraocular muscle fiber-type specificity of botulinum toxin. *Neurology* 51: 1093–1099, 1998.

**Stahl JS and James RA.** Comparing eye movements in *tottering* and *rocker*, murine P/Q calcium channel mutants. *Soc Neurosci Abstr* 29: 882.13, 2003.

**Stahl JS and James RA.** Effect of aging on compensatory eye movements of *tottering*, a murine CACNA1A mutant. *Soc Neurosci Abstr* 30: 411.12, 2004.

**Stahl JS and James RA.** Neural integrator function in murine CACNA1A mutants. *Ann NY Acad Sci* 1039: 580–582, 2005.

**Stahl JS and Simpson JI.** Dynamics of rabbit vestibular nucleus neurons and the influence of the flocculus. *J Neurophysiol* 73: 1396–1413, 1995.

**Stahl JS, van Alphen AM, and De Zeeuw CI.** A comparison of video and magnetic search coil recordings of mouse eye movements. *J Neurosci Methods* 99: 101–110, 2000.

**Stea A, Tomlinson WJ, Soong TW, Bourinet E, Dubel SJ, Vincent SR, and Snutch TP.** Localization and functional properties of a rat brain alpha 1A

calcium channel reflect similarities to neuronal Q- and P-type channels. *Proc Natl Acad Sci USA* 91: 10576–10580, 1994.

**Tan HS, van der Steen J, Simpson JI, and Collewijn H.** Three-dimensional organization of optokinetic responses in the rabbit. *J Neurophysiol* 69: 303–317, 1993.

**Tottene A, Fellin T, Pagnutti S, Luvisetto S, Striessnig J, Fletcher C, and Pietrobon D.** Familial hemiplegic migraine mutations increase $Ca^{2+}$ influx through single human $Ca_v2.1$ channels and decrease maximal $Ca_v2.1$ current density in neurons. *Proc Natl Acad Sci USA* 99: 13284–13289, 2002.

**van Alphen AM, Schepers T, Luo C, and De Zeeuw CI.** Motor performance and motor learning in lurcher mice. *Ann NY Acad Sci* 978: 413–424, 2002.

**van Alphen AM, Stahl JS, Koekkoek SKE, and De Zeeuw CI.** The dynamic characteristics of the mouse vestibulo-ocular and optokinetic response. *Brain Res* 890: 296–305, 2001.

**van der Steen J, Simpson JI, and Tan T.** Functional and anatomical organization of three-dimensional eye movements in rabbit cerebellar flocculus. *J Neurophysiol* 72: 31–46, 1994.

**van Neerven J, Pompeiano O, and Collewijn H.** Depression of the vestibulo-ocular and optokinetic responses by intrafloccular microinjection of GABA-A and GABA-B agonists in the rabbit. *Arch Ital Biol* 127: 243–263, 1989.

**Walker MF and Zee DS.** Directional abnormalities of vestibular and optokinetic responses in cerebellar disease. *Ann NY Acad Sci* 871: 205–220, 1999.

**Yuste R and Tank DW.** Dendritic integration in mammalian neurons, a century after Cajal. *Neuron* 16: 701–716, 1996.

**Zee DS, Walker MF, and Ramat S.** The cerebellar contribution to eye movements based upon lesions: binocular three-axis control and the translational vestibulo-ocular reflex. *Ann NY Acad Sci* 956: 178–189, 2002.

**Zhou YD, Turner TJ, and Dunlap K.** Enhanced G protein-dependent modulation of excitatory synaptic transmission in the cerebellum of the $Ca^{2+}$ channel-mutant mouse, *tottering*. *J Physiol* 547: 497–507, 2003.

**Zuo J, De Jager PL, Takahashi KA, Jiang W, Linden DJ, and Heintz N.** Neurodegeneration in Lurcher mice caused by mutation in delta2 glutamate receptor gene. *Nature* 388: 769–773, 1997.

**Zwingman TA, Frankel W, and Herrup K.** Two new mouse variants of the voltage dependent calcium channel subunit gene alpha1A. *Soc Neurosci Abstr* 24: 316.14, 2000.

**Zwingman TA, Neumann PE, Noebels JL, and Herrup K.** Rocker is a new variant of the voltage dependent calcium channel gene Cacna1a. *J Neurosci* 21: 1169–1178, 2001.